ADAS-EU R(10)PU01

ADAS-EU
ADAS for fusion in Europe

Grant: 224607

Adam Foster, Martin O'Mullane and Hugh Summers

Charge exchange spectroscopy for fusion plasmas

17 June 2010

Workpackages : 2.34
Category : DRAFT

Charge exchange spectroscopy for fusion plasmas

Adam Foster, Martin O'Mullane and Hugh Summers

Department of Physics, University of Strathclyde, Glasgow, UK

Abstract: *Charge exchange spectroscopy (CXS) using fast neutral beams has a history of nearly thirty years. CXS is now a principle diagnostic on most fusion machines of proven effectiveness. Most of this application has been to the bare nuclei of light elements of nuclear charge* $z_0 \leq 10$ *as the charge exchange receiver and with neutral deuterium,* D^0*, as the donor. Present and future application, with a view to ITER, is focussed on heavier elements - argon and above - and also on partially stripped receivers occuring towards the periphery of the plasma. The present work is concerned with re-examining and elaborating the older CXS models and with extension and critical reassessment of the fundamental atomic reaction database for heavier elements. The work comprises part of the the redesign/re-orientation of ADAS for heavy species and ITER . Therefore it also lays out the comprehensive atomic modelling and fundamental/derived data environment for medium/heavy species for fusion application which ADAS will support and on which further more refined developments will be made.*

Contents

Preface

This article is the first of a series of technical notes which are being prepared as useful extracts during the longer term construction of the next edition of the ADAS user manual[**?**]. As such it reflects the change in style, planned for the new manual. It is more book-like, examining and explaining in detail the physics basis behind the commitment to certain approaches in ADAS and how these work out in practice. The manual is technically detailed with extended appendices, however, this is ameliorated by much more emphasis on worked examples. That is to say the actual manoeuvres, adopted by experienced ADAS users in getting the atomic modelling into application scenarios will be mapped, rather as an expert system.

H P Summers
17 June 2010

Chapter 1

Introduction

Charge exchange spectroscopy (CXS) is a widely used diagnostic in fusion devices for ion temperature, plasma rotation and impurity concentrations of light elements such as helium, beryllium, carbon, oxygen and neon. These plasma parameters are obtained at the localised positions of the intersections of viewing lines and the line of the neutral beam (usually deuterium) which drives the initiating charge exchange reaction between the beam donor atom and the plasma impurity ion receiver. The neutral beam species is usually an isotope of hydrogen (deuterium at JET), but helium.and mixtures of helium and hydrogen can be used. The primary state selective charge transfer reaction with a deuterium beam *donor* atom in its ground state $D_b^0(1s)$ is

$$\mathcal{A}^{+z+1}(\gamma) + D_b^0(1s) \rightarrow \mathcal{A}^{+z}(\gamma, nlj) + D_b^+ \tag{1.1}$$

where $\mathcal{A}^{+z+1}(\gamma)$ is a plasma impurity initial *receiver* ion in state γ. With light element impurities in high temperature fusion devices, such as AUG and JET, the receiver ions in the confined central plasma are the bare nuclei of the respective elements. Capture is into excited Rydberg states characterised by nlj quantum numbers. These excited states are subject to redistributive collisions by electrons and positive ions (principally deuterons and other bare nuclei) in the plasma as

$$\mathcal{A}^{+z}(\gamma, nlj) + \left[\begin{array}{c} e \\ \mathcal{X}^{+z_0} \end{array} \right] \rightarrow \mathcal{A}^{+z}(\gamma, n'l'j') + \left[\begin{array}{c} e \\ \mathcal{X}^{+z_0} \end{array} \right] \tag{1.2}$$

where $\mathcal{X}^{+z_0}$ is a representative plasma impurity collider assumed in the fully ionised charge state z_0.. These reactions are in competition with radiative decay

$$\mathcal{A}^{+z}(\gamma, nlj) \rightarrow \mathcal{A}^{+z}(\gamma, n'l'j') + h\nu \tag{1.3}$$

The parent state γ is passive in these reactions. Charge exchange spectral line emission - which is the valence electron cascade emission following the initial capture into these highly excited principal quantum shells - spans a wide spectral range which includes the visible. The advantages of charge exchange spectroscopy lie in the spatial localisation, the active nature of the signals and the possibility of absolutely calibrated spectroscopy in the visible. An observed spectral intensity along a spectrometer line-of-sight intersecting the beam-plasma overlap volume is an unresolved superposition of transition arrays between principal quantum shells because of the high thermal Doppler broadening in the core of the plasma, as

$$I_{n \rightarrow n'} = \sum_{l,l',j,j'} I_{nlj \rightarrow n'l'j'}. \tag{1.4}$$

For notational simplicity the frozen parent state is omitted.

In the preparations and progress towards ITER, we look to the use of heavier control gases such such as argon and krypton, and heavy first wall and marker species such as tungsten, which we shall wish to measure in the plasma. An interesting development occurs with charge exchange spectroscopy of argon. Ar^{+18} is the dominant ion in the confined plasma of JET, so that Ar^{17} the expected active CXS emitter, but charge exchange emission following capture by the ions Ar^{+17} and Ar^{+16} occuring towards the edge of the plasma is also observed. In lower temperature devices such

as AUG and MAST, the Ar^{+16} stage extends into the plasma centre. Simultaneous CXS measurement from all three stages gives shell localisation along the beam path and therefore a direct indicator of impurity ion transport.

Broad considerations of z-scaling suggest a worsening of the conditions for charge exchange spectroscopy for heavier more highly ionised species. The dominant charge exchange capture from $D^0(1s)$ to an ion A^{+z} is into shells $n \sim z^{3/4}$ and the visible emission is from n-shells $\sim 2z^{3/4}$. For $D^0(n = 2)$ as the donor, the dominant capture is into shells $\sim 2z^{3/4}$. So modelling must cope with many high n-shells. Whereas total charge exchange cross-sections scale approximately as $\sim z$, heavy species impurity concentrations which can be tolerated in fusion devices (because of their efficiency as radiators) must be reduced as $\sim z^{-3}$ and the net capture is spread amongst more lines in the visible, scaling as $\sim z$. Also for a heavy species in the core plasma at any position, a range of ionisation stages will be present as receivers, increasing the dispersion amongst a range of lines and in particular in the visible. Detection methods may in the future enable simultaneous measure of many charge exchange lines in the visible and counter to some extent the dilution effect amongst many lines. Since the receiver ion is a thermal species in the plasma with its emitted lines thermally Doppler broadened, the mass dependence recovers a factor $\sim z^{1/2}$ from the line width in measurement. But overall therefore, we must expect the opportunities for individual line CXS to decrease as we move to heavier species than argon - for which individual line CXS is evidently practicable. This does not of itself mean that charge exchange spectroscopy with heavy species can be ignored. A weak, very many line, dispersed signal at the Bremsstrahlung fluctuation level is clearly an issue for Bremsstrahlung and z_{eff} background measurement and for the extraction of other broad, weak, active CXS features such as slowing alpha particles. The expected CXS signals of heavier species are therefore important and worthy of study as both identifiable lines and as a background correction - in both circumstances retaining the advantage of being active signals and relatively accurately predictable theoretically. The description of a new ADAS development to enable predictions of such CXS signals from any element, at a baseline level of low/moderate precision, suitable for initial surveys for relevance, is a purpose of this technical report. The report will also develop methods allowing targetted improvement of modelling for selected species to ADAS level 1 and level 2 precisions.

The ADAS provision for light element charge exchange analysis comprises three parts: a database of fundamental state selective charge exchange cross-section data of data format *adf01*; a set of collisional-radiative programs for computing receiver excited state populations, emission measures and effective emission coefficients in ADAS code series *adas3xx*; a database of effective emission coefficients in economised tabulations of data format *adf12* for fast look-up in experimental analyses . For this heavy species development, the same broad organisation is followed but with some substantial developments and new codes. These are described in the following chapters. Chapter 2 explains the mathematical background of the collisional-radiative population calculation approaches. Chapter 3 addresses calculation and procurement of the fundamental state charge exchange and associated ion impact excitation cross-sections. describes the procedures which are used for establishment of the *adf01* database. Chapter 4 builds a univeral solution for arbitary heavy species ions at baseline quality. collisional-radiative population calculation approaches and the new codes provided for their execution. Chapter 5 gives an overview of the additional codes and data formats being made available in ADAS to fulfill the level 1 and level 2 objectives of this report. Attention is also drawn to the ADAS heavy species feature and superfeature emissivity approach which has relevance to charge exchange spectroscopy, but does not have an ADAS equivalent in the earlier light element work. There is an extensive appendix detailing the precise structure of the data formats and the parameters and calling sequences of the various codes.

Chapter 2

Collision-radiative modelling environments

In principle, collisional-radiative modelling for charge exchange spectroscopy driven by beams follows a similar pattern to emissivity calculations in thermal plasma, but with an extra primary driving term. Consider then the populations of ionisation stage z of an element $\mathcal{A}$. This stage represents the recombined receiver system. In the scenarios reviewed in chapter 1, partially ionised receiver ions are allowed and so the recombined receiver is not necessarily a hydrogenic system. Adopting the usual generalised collisional radiative, *GCR*, picture, its populations may be separated into the metastable populations N_ρ^{+z}, indexed by the Greek letter ρ, and ordinary excited populations N_i^{+z}, indexed by the Roman letter i. The stage z has adjacent stages $z-1$ and $z+1$, its *child* and *parent*, with metastable populations labelled as N_μ^{+z-1} and N_ν^{+z+1} respectively. The time-dependent equations 2.1 of the populations in thermal plasma without beams comprise the left hand side of 2.1 and the first part of the right-hand-side.

$$\frac{d}{dt}\begin{bmatrix} N_\mu^{+z-1} \\ N_\rho^{+z} \\ N_i^{+z} \\ N_\nu^{+z+1} \end{bmatrix} = \begin{bmatrix} \mathcal{C}_{\mu\mu'} & N_e\mathcal{R}_{\mu\sigma} & 0 & 0 \\ N_e\mathcal{S}_{\rho\mu'} & C_{\rho\sigma} & C_{\rho j} & N_e r_{\rho\nu'} \\ 0 & C_{i\sigma} & C_{ij} & N_e r_{i\nu'} \\ 0 & N_e S_{\nu\sigma} & N_e S_{\nu j} & \mathcal{C}_{\nu\nu'} \end{bmatrix} \begin{bmatrix} N_{\mu'}^{+z-1} \\ N_\sigma^{+z} \\ N_j^{+z} \\ N_{\nu'}^{+z+1} \end{bmatrix} + \sum_{b,p\geq 1} \mathcal{N}_p^{(b)} \begin{bmatrix} \mathcal{R}_{p;\,\mu\sigma}^{(b)} & 0 & 0 \\ -\sum_\mu \mathcal{R}_{p;\,\mu\sigma}^{(b)} & 0 & r_{1p;\,\rho\nu'}^{(b)} \\ 0 & 0 & r_{1p;\,i\nu'}^{(b)} \\ 0 & 0 & -\sum_\rho r_{1p;\,\rho\nu'}^{(b)} - \sum_i r_{1p;\,i\nu'}^{(b)} \end{bmatrix} \begin{bmatrix} N_\sigma^{+z} \\ N_j^{+z} \\ N_{\nu'}^{+z+1} \end{bmatrix} \tag{2.1}$$

Equations 2.1 are written in matrix/suffix form[5], where we have omitted coupling to more distant ionisation stages. We show the excited populations of the stage z explicitly, whereas the quasi-static *GCR* condensation process (see below) has already been applied to stages $z+1$ and $z-1$. Thus they only show their dominant metastable populations and the effective coefficients which couple them. The elements $C_{\rho\sigma}$, C_{ij} etc. represent radiative plus thermal collisional processes. The collisional processes include collisional transitions caused by Maxwellian electron colliders, but also Maxwellian positive ions. It can be helpful to consider the latter as being just one species, z_{eff} colliders, or posssible a particular bare nucleus collider $\mathcal{X}^{z_0}$ and a second z'_{eff} collider representing all other positive ion types. So typically $C_{ij} = A_{j\to i} + N_e q_{j\to i}^{(e)}(T_e) + N_{zeff} q_{j\to i}^{(zeff)}(T_{zeff})$. Note that the on-diagonal elements of C and $\mathcal{C}$ are -ve quantities and include electron impact ionisation and positive ion impact ionisation losses. Thus, typically $N_e S_{\nu\sigma} = N_e S_{\sigma\to\nu}^{(e)}(T_e) + N_{zeff} S_{\sigma\to\nu}^{(zeff)}(T_{zeff})$. This quantity is contained negatively in the diagonal element $C_{\sigma\sigma}$ and the column sums of the elements of the whole matrix are zero.

The second part on the right-hand side of equations 2.1 is the extra contribution driven by the neutral beam populations, called $\mathcal{N}_p^{(b)}$ here (distinguishing different beam species b and states of these species p). This driving term arises from a non-thermal population (the donor) which is not in full statistical balance with the receiver populations. There are no matching inverse reactions as the ionised beam particles exit the reaction zone immediately on formation. That is, there is no mechanism for recreation of the beam population. Unlike the reactions of the first part on the right-hand side of equations 2.1, the beam speed contributes to the relative velocity of the reaction participants here. The $r^{(b)}$

[5] In the following equations summation convention over repeated indices is adopted.

are state selective charge exchange recombination coefficients. Note that the indices before the semi-colon in $r^{(b)}_{1p;\,\rho\nu'}$ relate to the donor state, with the first index refering to the final (ionised) donor state and the second index to the initial (un-ionised) donor state. The indices following the semi-colon relate to the receiver, with the first refering to the recombined receiver and the second to the initial receiver. The metastable initial receiver states are the only ones significantly populated and therefore contributing to charge exchange recombination. The equations are actually complete only for the stage z. Note that we have not shown explicitly the ordinary populations of stages $z-1$ and $z+1$ and that some of the sub-matrices are shown as script letters (eg. $\mathcal{C}_{\mu\mu'}$ and $\mathcal{R}_{\mu\sigma}$) whereas others are shown as standard letters (eg. $C_{\rho\sigma}$ and $S_{\nu j}$). Technically, this is because a 'quasi-static' assumption has been made about the ordinary populations of the stages $z-1$ and $z+1$ and the influence of their ordinary populations has been condensed onto their metastable populations.

The specification of the beam donor, $\mathcal{N}^{(b)}$ in equations 2.1 is abbreviated. It has its own collisional-radiative picture and population structure so that $\mathcal{N}^{(b)}_p$ should in fact distinguish ground and excited donor populations ($\mathcal{N}^{(b)}_1$ and $\mathcal{N}^{(b)}_p$ with $p > 1$) . Also the connection with the ionised beam population $\mathcal{N}^{(b)+}$ needs to be established. Completeness of the picture from the perspective of the beam donor requires the equation set

$$\frac{d}{dt}\begin{bmatrix} \mathcal{N}^{(b)}_1 \\ \mathcal{N}^{(b)}_p \\ \mathcal{N}^{(b)+}_1 \end{bmatrix} = \begin{bmatrix} C^{(e)}_{11} & C^{(e)}_{1q} \\ C^{(e)}_{p1} & C^{(e)}_{pq} \\ N_e S^{(e)}_{11} & N_e S^{(e)}_{1q} \end{bmatrix} \begin{bmatrix} \mathcal{N}^{(b)}_1 \\ \mathcal{N}^{(b)}_q \end{bmatrix} + \begin{bmatrix} C^{(b,ion)}_{11} & C^{(b,ion)}_{1q} \\ C^{(b,ion)}_{p1} & C^{(b,ion)}_{pq} \\ N^{(ion)}(S^{(b,ion)}_{11} + R^{(b,ion)}_{11}) & N^{(ion)}(S^{(b,ion)}_{1q} + R^{(b,ion)}_{1q}) \end{bmatrix} \begin{bmatrix} \mathcal{N}^{(b)}_1 \\ \mathcal{N}^{(b)}_q \end{bmatrix} \tag{2.2}$$

where

$$\begin{array}{lll} N^{(ion)}R^{(b,ion)}_{11} = \sum_{\nu',z,\rho} r^{(b)}_{11;\,\rho\nu'} N^{+z+1}_{\nu'} & ; & N^{(ion)}S^{(b,ion)}_{11} = \sum_{\nu',z,\rho} s^{(b)}_{11;\,\rho\nu'} N^{+z+1}_{\nu'} \\ N^{(ion)}R^{(b,ion)}_{1q} = \sum_{\nu',z,\rho} r^{(b)}_{1q;\,\rho\nu'} N^{+z+1}_{\nu'} & ; & N^{(ion)}S^{(b,ion)}_{1q} = \sum_{\nu',z,\rho} s^{(b)}_{1q;\,\rho\nu'} N^{+z+1}_{\nu'} \end{array} \tag{2.3}$$

with

$$N^{(ion)} = \sum_{\nu',z,\rho} N^{+z+1}_{\nu'} \tag{2.4}$$

In equations 2.2 the collisional-radiative matrix elements C are not the same as those in equations 2.1. The distinction $C^{(z)}$ and $C^{(b)}$ should be made, but at the expense of even more superscript/subscript complexity. The ionised beam population $\mathcal{N}^{(b)+}_1$ is not fully statistically coupled to the neutral beam populations. That is because the ionised beam population responds to the magnetic field and moves independently away from the local beam plasma interaction zone. There is only a pathway from neutral beam to ionised beam and no reverse path in the model. The excited state populations of the beam, with the assumption of quasi-equilibrium are obtained by setting the time-derivative to zero in equation 2.2 obtaining

$$\mathcal{N}^{(b)}_q = -[C_{qp} - (S^{(b,ion)}_{1p'} + R^{(b)}_{1p'})_{p'=p}\delta_{qp}]^{-1} C_{p1} \mathcal{N}^{(b)}_1 \tag{2.5}$$

Back substitution in equation 2.2 gives

$$\frac{d\mathcal{N}^{(b)}_1}{dt} = -N_e \mathcal{S}^{(b)}_{11} \mathcal{N}^{(b)}_1 \tag{2.6}$$

where

$$\mathcal{S}^{(b)}_{11} = [-C_{11} + S^{(b,ion)}_{11} + R^{(b)}_{11} + C_{1q}[C_{qp} - (S^{(b,ion)}_{1p'} + R^{(b)}_{1p'})_{p'=p}\delta_{qp}]^{-1} C_{p1}]/N_e \tag{2.7}$$

is the beam stopping coefficient. It is conventional to write the coefficient in terms of the electron density N_e. Beam stopping (equation 2.6) and beam emission (derived from equation 2.4) is the subject of a separate report, ADAS-EU R(10)PU04.

Returning to equations 2.1 and and making the quasi-static assumption for the populations $N^{(+z)}_i$, then

$$N^{(+z)}_j = -C^{-1}_{ji} C_{i\sigma} N^{+z}_\sigma - N_e C^{-1}_{ji} r_{i\nu'} n N^{+z+1}_{\nu'} + \sum_{b,p\geq 1} C^{-1}_{ji} r^{(b)}_{i\nu'} N^{(b)}_p N^{(+z+1)}_{\nu'} \tag{2.8}$$

and equations 2.1 reduce to

$$\frac{d}{dt}\begin{bmatrix} N^{+z-1}_\mu \\ N^{+z}_\rho \\ N^{+z+1}_\nu \end{bmatrix} = \begin{bmatrix} \mathcal{C}_{\mu\mu'} & N_e\mathcal{R}_{\mu\sigma} & 0 \\ N_e\mathcal{S}_{\rho\mu'} & \mathcal{C}_{\rho\sigma} & \mathcal{R}_{\rho\nu'} \\ 0 & N_e\mathcal{S}_{\nu\sigma} & \mathcal{C}_{\nu\nu'} \end{bmatrix} \begin{bmatrix} N^{+z-1}_{\mu'} \\ N^{+z}_\sigma \\ N^{+z+1}_{\nu'} \end{bmatrix} + \sum_{b,p\geq 1} \mathcal{N}^{(b)}_p \begin{bmatrix} \mathcal{R}^{(b)}_{p;\,\mu\sigma} & 0 \\ -\sum_\mu \mathcal{R}^{(b)}_{p;\,\mu\sigma} & \mathcal{R}_{p;\,\rho\nu'} \\ 0 & -\sum_\rho \mathcal{R}_{p;\,\rho\nu'} \end{bmatrix} \begin{bmatrix} N^{+z}_\sigma \\ N^{+z+1}_{\nu'} \end{bmatrix} \tag{2.9}$$

In equations 2.8 for the $N_j^{(+z)}$, the first term is the usual collisional-radiative source terms (that is collisional excitation driven by the metastables $N_\sigma^{(+z)}$, and free electron capture driven by the metastables $N_{\nu'}^{+z+1}$ of the stage above. The last term is the charge exchange recombination contribution which matters here and leads on to the charge exchange line emissivities. The last term in equations 2.9 give the extra *GCR* source terms which should enter the transport/ionisation equations for the dominant metastable populations in regions where they are exposed to the beams.

Charge exchange from a fast beam donor is generally to highly excited states of the receiver. To a very good approximation, the ordinary excited levels (not metastable levels) of the recombined receiver ion $\mathcal{A}^{+z}$ may be viewed as composed of a single outer valence electron weakly coupled to a core state. The core or parent state is a metastable of the $\mathcal{A}^{+z+1}$ initial receiver, such as $\mathcal{A}_\nu^{+z+1}$. It is helpful to consider three representations of the collisional-radiative matrices, of progressively greater excited level span but of progressively coarser resolution.

$$\left[\begin{array}{c} C_{ik}^{(ic)} \end{array}\right], \left[\begin{array}{cc} C_{\bar{i}\bar{k}}^{(ca)} & C_{\bar{i}k'}^{(ca)} \\ C_{i'\bar{k}}^{(ca)} & C_{i'k'}^{(ca)} \end{array}\right], \left[\begin{array}{ccc} C_{\bar{\bar{i}}\bar{\bar{k}}}^{(bn)} & C_{\bar{\bar{i}}\bar{k}'}^{(bn)} & C_{\bar{\bar{i}}k''}^{(bn)} \\ C_{\bar{i}'\bar{\bar{k}}}^{(bn)} & C_{\bar{i}'\bar{k}'}^{(bn)} & C_{\bar{i}'k''}^{(bn)} \\ C_{i''\bar{\bar{k}}}^{(bn)} & C_{i''\bar{k}'}^{(bn)} & C_{i''k''}^{(bn)} \end{array}\right] \tag{2.10}$$

The different resolutions are called *ic*, *ca* and *bn* in ADAS paralance. Here $i \equiv \gamma_\nu, n_i l_i j_i$, $\bar{i} \equiv \gamma_\nu, n_i l_i$ and $\bar{\bar{i}} \equiv \gamma_\nu, n_i$. Partitioning delimits the progressively extending ranges. The notation means that $C_{\bar{i}\bar{j}}^{(ca)}$ spans the same range of levels as $C_{ij}^{(ic)}$, but in the former case the components are bundled-up for whole valence electron shells (configurations), while in the latter the levels are fully resolved. Again $C_{i'j'}^{(ca)}$ and $C_{\bar{i}'\bar{j}'}^{(bn)}$ span the same range of valence electron shells , but in the latter case are bundled-up into valence electron principal quantum shells. It is helpful to recognise regions of different behaviour of the excited population structure delimited by critical n-values. The lowest accessible n-shell, is denoted by n_0. n_1 is the n-shell above which the assumption of Rydberg behaviour outside a coupled core is appropriate. For $n < n_1$ the core is coupled to the valence electron and fully resolved $(J_\nu)nljJ$ state populations are distinguished. For compactness, the core state γ_ν is represented only by its total angular momentum quantum numbers as (J_ν). The core is essentially passive in the present work apart from some modest perturbation of valence electron binding energies. For $n \geq n_1$ the populations summed over J may be used without significant error, that is bundled states $(J_\nu)nlj$. Denote the reciprocal radiative lifetime for state $(J_\nu)nlj$ by $A_{(J_\nu)nlj}$ so that

$$A_{(J_\nu)nlj} = \sum_{n'<n,l',j'} A_{(J_\nu)nlj\to(J_\nu)n'l'j'} \tag{2.11}$$

The associated reciprocal radiative lifetimes of the bundled states $(J_\nu)nl$ and $(J_\nu)n$ (assuming statistically weighted sub-populations) are also relevant. That is

$$A_{(J_\nu)n} = \frac{1}{2n^2}\sum_l A_{(J_\nu)nl} = \sum_l \frac{1}{2(2l+1)}\sum_j (2j+1)A_{(J_\nu)nlj} \tag{2.12}$$

Consider the n-shell for which

$$\begin{aligned} max(A_{(J_\nu)nlj}) \quad \sim \quad & N_e(q^{(e)}_{(J_\nu)nlj\to(J_\nu)nl+1,j+1}(T_e) + q^{(e)}_{(J_p)nlj\to(J_p)nl-1,j-1}(T_e)) + \\ & N_{zeff}(q^{(zeff)}_{(J_\nu)nlj\to(J_\nu)nl+1,j+1}(T_{zeff}) + q^{(zeff)}_{(J_p)nlj\to(J_p)nl-1,j-1}(T_{zeff})) \end{aligned} \tag{2.13}$$

This defines $n = n_c^{(lj)}$ which marks the centre of the regime in which lj sub-state collisional redistribution within an n-shell is in competition with radiative cascade. This is effectively the same regime as defined in a *ca* picture, that is

$$\begin{aligned} A_{(J_\nu)nl} \quad \sim \quad & N_e(q^{(e)}_{(J_\nu)nl\to(J_\nu)nl+1}(T_e) + q^{(e)}_{(J_p)nl\to(J_p)nl-1}(T_e)) + \\ & N_{zeff}(q^{(zeff)}_{(J_\nu)nl\to(J_\nu)nl+1}(T_{zeff}) + q^{(zeff)}_{(J_p)nl\to(J_p)nl-1}(T_{zeff})) \end{aligned} \tag{2.14}$$

with critical n-shell $n_c^{(ca)}$ since it is the larger energy difference $(J_\nu)nlj \to (J_\nu)nl \pm 1j \pm 1$ transitions which block redistribution within an n-shell and these energy differences are close to the term centroid energy differences.

Redistribution between n-shells occurs when

$$\begin{aligned} A_{(J_\nu)n} \quad \sim \quad & N_e(q^{(e)}_{(J_\nu)n\to(J_\nu)n+1}(T_e) + q^{(e)}_{(J_p)n\to(J_p)n-1}(T_e)) + \\ & N_{zeff}(q^{(zeff)}_{(J_\nu)n\to(J_\nu)n+1}(T_{zeff}) + q^{(zeff)}_{(J_p)n\to(J_p)n-1}(T_{zeff})) \end{aligned} \tag{2.15}$$

defining a final critical n-shell $n_c^{(bn)}$. It is at much higher n-shells than lj redistribution, so the bn picture is appropriate for them. Once distribution between n-shells is open, the populations easily ionise in a step-wise manner and any over-population by charge exchange capture is eliminated. For computational implementation, it is necessary to establish the critical n-values and then define ranges around these critical n-values to which the appropriate tuned collisional radiative population model may be applied. Some broad scalings are to be noted. Consider the recombined ion of charge z, which is the CXS emitter, ion colliders of charge $zeff$ and of atomic mass number M_{zeff}. Also denote an equivalent hydrogen emitter case ($z+1=1$) by the superscript H with a proton collider ($zeff=1$) by superscript p. Relations 2.16 and 2.17 make the assumption that both electron and ion collisions are in the high energy Born/Bethe regime with ion and electron temperatures the same. Then the electron collisionality is reduced by the square root of the mass factor with respect to the ions. This assumption depends on the smallness of the ratio of the transition energy to the collider mean energy which breaks down for transitions between lower n-shells and lower collider temperatures.

$$A_n^{(z)} \sim (z+1)^4 \left(\frac{n_c}{n}\right)^3 A_{n_c}^H \quad \text{and} \quad \mathrm{q}_{\mathrm{n}\to\mathrm{n}'}^{(\mathrm{zeff,z})} \sim \frac{\mathrm{zeff}^2}{(\mathrm{z}+1)^3}\left(\frac{\mathrm{n}}{\mathrm{n_c}}\right)^4 \mathrm{q}_{\mathrm{n_c}\to\mathrm{n_c'}}^{(\mathrm{H,p})}. \tag{2.16}$$

Since $N_e = zeff\, N^{(zeff)}$ and $q_{n_c\to n_c'}^{(H,p)} \sim \sqrt{\frac{M_{zeff}}{m_e}} q_{n_c\to n_c'}^{(H,e)}$, n_c is determined fom the equation

$$\left(\frac{zeff^2}{(z+1)^7}\right) N^{(zeff)} \sqrt{\frac{M_{zeff}}{m_e}} \left(1 + \frac{1}{zeff}\sqrt{\frac{m_e}{M_{zeff}}}\right) = 1 \tag{2.17}$$

Choosing an upper bound criterion as the radiative lifetime being a factor $1/F$ longer than the collisional lifetime, then the upper boundary n-value is obtained from $(n_c/n)^7 = F$. Similar scaling relationships may be inferred for the l-redistribution case of equation 2.14, but the collisional transitions are then within an n-shell. Transition energies are then much smaller than in the n-shell changing case and the region of validity of the above assumptions is much wider. A full evaluation requires actual collisional rates and transition probabilities. ADAS has extensive Fortran subroutines and IDL procedures for evaluation of the radiative transition probabilities (*ahnn1.for* etc.) and the collisional rate coefficients (*ndegcol.for* etc.). Practical use of these will be illustrated in chapter 5, while the full descriptors are in appendices B and C.

Historically, in ADAS series 3, the codes ADAS306, ADAS307, ADAS308 and ADAS309 have provided the modelling of the populations of the excited states for light element bare nucleus and helium-like charge exchange receivers. In the following sections, we re-examine the theoretical basis of these codes and develop the extensions which are required to cope with arbitrary species.

2.1 The n-shell redistributive/cascade model

Thus the population structure after electron capture is that of a one-electron system, and since the visible line emissivities are from quite highly excited principal quantum shells, it can (apart from the s orbitals) be viewed as hydrogenic. The s orbital population contributions are a small part of the essentially unresolvable $n \to n'$ transition array emisssivities. Nonetheless l and lj fine structure populations are not in general statistical for the upper n of visible transitions, but are determined by a competion between l-redistribution within the n-shell, driven by ion collisions and radiative cascade both as a depopulating mechanism downwards to n-shells below n and as a populating mechanism from n-shells above n. As well as purely theoretical calculation of effective charge exchange driven $n \to n'$ emissivities, this model allowed special analysis of several observed charge exchange lines in terms of effective emission measure and the quality of direct charge exchange capture cross-sections into n-shells.

2.1.1 Effective emission coefficients

2.1.2 Average emission measure and spectral analysis

2.2 Extending the model scope

2.2.1 The bundle-n model

For heavy specie partially ionised receivers in visible spectroscopy, we must be more concerned with very high n-shells, possibly very large cascading contributions from many yet higher n-shells and the proper matching of these high n-shell populations into the continuum and the residual ionised state. Evidently the parent core is potentially more perturbing of the highly excited captured electron and also the electrons return with a role to play in redistribution between n-shells and in ionising collisions. Cleary the most complete picture is of a bundled-n population $(\gamma_\nu J_\nu)n$ model at very high n-shells merging smoothly into an $(\gamma_\nu J_\nu)nl$, $(\gamma_\nu J_\nu)nlj$ and finally $(\gamma_\nu J_\nu)nljJ$ at low n-shells. For the present baseline survey, we are going to ignore these lower level sophistications and suppose that the bundle-n picture is valid everywhere. We anticipate only moderate error in this assumption, a situation which can be improved if necessary at a later stage.

Let $\mathcal{A}^{+z_1}$ denote the recombining ion and $\mathcal{A}^{+z_1-1}$ the recombined ion so that $z = z_1 - 1$ is the ion charge of the latter. z_1 is the effective ion charge and takes the place of the nuclear charge in the reduction of hydrogenic rate coefficients to compact forms in the statistical balance equations. Also introduce bundled populations

$$N_{\nu,n} \equiv N_{(\gamma_\nu J_\nu),n} = \sum_{l,j,J} N_{(\gamma_\nu J_\nu),nljJ} \tag{2.18}$$

and the assumption that

$$N_{\nu,nljJ} = \frac{(2J+1)}{(2J_\nu+1)(2j+1)} N_{\nu,nlj} = \frac{(2J+1)}{(2J_\nu+1)(2l+1)} N_{\nu,nl} = \frac{(2J+1)}{(2J_\nu+1)n^2} N_{\nu,n}. \tag{2.19}$$

The bundling is based on the observation that the largest collision cross-sections are those for which $n = n'$ and $l = l' \pm 1$. For these cases the transition energy is small (effectively zero for hydrogen or hydrogenic ions) and the cross-sections are so substantial for electron/ion densities of relevance for fusion allowing the approximation of assuming relative statistical population for the ljJ sub-states. The assumption is weakest for low lying populations of states with core penetrating valence electron orbitals and we expect spin system breakdown for high nl states progressively at lower n and l and for increasing ion charge z. In the bundle-n model, only equilibrium populations of complete n-shells for a given parent need be evaluated, which are the solutions of the statistical balance equations

$$\begin{aligned}
& \textstyle\sum_{n'=n+1}^{\infty}[A_{n'\to n} + N_e q^{(e)}_{n'\to n} + N_p q^{(p)}_{n'\to n} + \sum_{imp} N_{imp} q^{(imp)}_{n'\to n}] N_{\nu,n'} \\
+ \quad & \textstyle\sum_{n''=n_0}^{n-1}[N_e q^{(e)}_{n''\to n} + N_p q^{(p)}_{n''\to n} + \sum_{imp} N_{imp} q^{(imp)}_{n''\to n}] N_{\nu,n''} \\
+ \quad & \left[N_e N^+_\nu \alpha^{(r)}_n + N_e N^+_\nu \alpha^{(d)}_n + N^2_e N^+_\nu \alpha^{(3)}_n + N_H N^+_\nu \alpha^{(CX)}_n\right] \\
= \quad & \{\textstyle\sum_{n'=n+1}^{\infty}[N_e q^{(e)}_{n\to n'} + N_p q^{(p)}_{n\to n''} + \sum_{imp} N_{imp} q^{(imp)}_{n\to n''}] \\
+ \quad & \textstyle\sum_{n''=n_0}^{n-1}[A_{n\to n''} + N_e q^{(e)}_{n\to n''} + N_p q^{(p)}_{n\to n''} + \sum_{imp} N_{imp} q^{(imp)}_{n\to n''}] \\
+ \quad & N_e q^{(e)}_{n\to\epsilon} + N_p q^{(p)}_{n\to\epsilon} + \textstyle\sum_{imp} N_{imp} q^{(imp)}_{n\to\epsilon} + \sum_{\nu'} A^a_{\nu,nS\to\nu'}\} N_{\nu,n}.
\end{aligned} \tag{2.20}$$

N^+_ν is the population of the parent ion $\mathcal{A}^{+z_1}_\nu$, N_e is the free electron density and N_p the free proton density, A is the usual Einstein coefficient, $q^{(e)}$, $q^{(p)}$ and $q^{(imp)}$ denote collisional rate coefficients due to electrons, protons and impurity ions, $\alpha^{(r)}_n$, $\alpha^{(d)}_n$ and $\alpha^{(3)}_n$ denote radiative, dielectronic and three-body recombination coefficients respectively, $\alpha^{(CX)}_n$ denotes the charge exchange direct capture rate coefficient and $q^{(e)}_{n\to\epsilon}$, $q^{(p)}_{n\to\epsilon}$ and $q^{(imp)}_{n\to\epsilon}$ denote collisional ionisation rate coefficients due to electrons, protons and impurity ions respectively. For complex ions, there are separate systems of equations for each parent and one such equation for each value of n from the lowest allowed n-shell n_0 for the parent to ∞.

For hydrogenic ions it was advantageous to write the statistical equations in terms of Saha-Boltzmann deviation

factors. This remains true for complex ions but the definition must be generalised. The deviation $b_{\nu,nS}$ is defined by

$$N_{\nu,n} = N_e N_\nu^+ 8 \left(\frac{\pi a_0^2 I_H}{kT_e} \right)^{3/2} \frac{\omega_{\nu,n}}{2\omega_\nu} \exp(I_{\nu,n}/kT_e) b_{\nu,n}. \tag{2.21}$$

That is $b_{\nu,n}$ is specified with respect to the parent ion state $\mathcal{A}_\nu^{+z_1}$, and the ionisation energy $I_{\nu,n}$ is also referred to that parent. Note that $\omega_{\nu,n} = n^2\omega_\nu$ where $\omega_\nu = (2J_\nu + 1)$ is the parent statistical weight. It is convenient to introduce $c_{\nu,n} = b_{\nu,n} - 1$ and scaled temperatures and densities

$$\begin{aligned} \theta_e &= \left(\frac{kT_e}{I_H} \right) \frac{1}{z_1^2} \\ \rho_e &= 2^5 \sqrt{\frac{\pi}{3}} \frac{\pi a_0^2}{\alpha^3} \frac{N_e}{z_1^7} \end{aligned} \tag{2.22}$$

with similar forms for the proton temperature and density. In these terms the statistical balance equations become particularly suitable for calculation.

The resulting population structure has linear independent contributions driven from the ground state of the recombined receiver, (the *excitation part*), from free electron capture by the recombining receiver, (the *recombination part*) and by from neutral beam charge exchange capture by the recombining receiver, (the *charge exchange part*). Thus the $b_{nu,n}$ factor may be expressed as

$$b_{\nu,n} = f_n^{(1)}(N_{\nu,1}/Ne) + f_n^{(2)} + f_n^{(3)}(N_H/Ne) \tag{2.23}$$

where the f_ns are functions of the electron, proton and plasma impurity ion temperatures and densities. $f_n^{(3)}$ is the part of the population due to charge transfer and so gives the charge exchange line emissivities as

$$\epsilon_{n\to n'} = A_{n\to n'} f_n^{(3)} N_n^{(saha)}/NeN_\nu^+ \tag{2.24}$$

2.2.2 The bundle-nl model

2.3 Condensation, projection and inversion for advanced charge exchange modelling

Chapter 3

Extending the fundamental charge exchange cross-section calculations

3.1 Comparison of methods

3.2 State selective ion impact cross-sections

3.3 Lifting the ADAS fundamental charge exchange cross-section database

Chapter 4

A universal baseline of fundamental charge exchange data

State selective charge exchange cross-section data in the energy regime of fusion heating and daisgnostic beams is largely lacking for receivers above charge charge 18 (Ar^{+18}). However, charge exchange cross-sections for capture from the ground $1s$ state of a neutral hydrogen isotope donor in the moderate to high energy regime ($E_{cm} \gtrsim$ 10 keV/amu) have some characteristic behaviours which are helpful for establishment of a preliminary database of medium/heavy species, sufficient to focus further work. For the total capture, that is charge exchange summed over all receiver substates, the cross-section is almost independent of energy up to $E_{cm} \sim 30$ keV/amu above which it changes over to the Born high energy behaviour. The latter is formally $\sigma_{tot} \sim E_{cm}^{11/2}$, but is close to $\sigma_{tot} \sim E_{cm}^{-4}$ up to $E_{cm} \sim 300$ keV/amu which covers the relevant fusion neutral beam regime. At low energy, the flat behaviour of the cross-section is due to the availability of quasi-resonant n-shells of the receiver for higher charged receivers ($z_r \gtrsim 4$) so that there is no endothermic threshold. The total cross-section can safely be treated as flat down to energies $E_{cm} \sim 1$ keV/amu. The total cross-section scales broadly with the receiver ion charge $\sigma_{tot} \sim z_r^1$ in terms of a weakly scaled collision energy $E_{cm} \sim z_r^{1/4}$. The same behaviour is shown for capture from the $n = 2$ shell of a neutral hydrogen donor, but the switch between the low and high energy behaviour occurs at lower energy $E_{cm} \sim 10$ keV/amu.

The n-shell selective partial cross-sections are also characteristic, as illustrated in figure 4.1a. σ_n is a maximum for some excited principal quantum shell n_{crit} falling steeply for $n < n_{crit}$ and, at $n > n_{crit}$ (the so-called *subdominant states*) falling with a collision energy dependent behaviour. The asymptotic slope as a function of n is less steep at higher E_{cm} becoming asymptotically $\sim E_{cm}^{-3}$. It is to be noted that the principal quantum shells of receiver transitions which appear at visible wavelengths are from upper n-shells $\sim 2 \times n_{crit}$, so the subdominant region is of greatest importance for charge exchange spectroscopy. Again, a z_r scaling is evident, in particular, $n_{crit} \sim z_r^{3/4}$ for the $1s$ hydrogen donor state. For the $n = 2$ hydrogen donor state, the dominant capture is into $2 \times n_{crit}$. This means that the $n = 2$ hydrogen donor directly targets the receiver n-shells yielding visible transitions. For light element receivers, at usual primary beam fraction energies, the subdominant $n = 1$ capture exceeds the dominant $n = 2$ capture once the excited state population balance of the neutral hydrogen beam donor is taken into account. The competition is more fine for heavier species and so it is necessary to address both donor states in this work. The nl-shell selective partial cross-section behaviour is illustrated in figure 4.1b. for a given n-shell, σ_{nl} is a maximum for some l_{crit} with $l_{crit} \sim n_{crit}$. That is l_{crit} is effectively independent of n. For $l < l_{crit}$, the partial cross-section increases with l as $\sigma_{nl} \sim (2l + 1)$ and for $l > l_{crit}$, σ_{nl} falls exponentially. This work will present a method used to derive a universal scaling curve for charge exchange cross sections based on existing data. This can then be used to obtain cross sections for any recombining ion, $\mathcal{A}^{+z_r}$, and coupled with other codes within ADAS to predict the cascade emission for this ion. A final point to note is that for heavy species receivers in highly ionised states, the fact that n_{crit} is quite large (already $n \sim 6$ for a Ne^{+10} receiver) and $l_{crit} \sim n_{crit}$ means that the core of a partially ionised receiver is of little significance in the collision process. Thus to a good approximation, it is the charge of the receiver ion which is important, not its nuclear charge.

ADAS has a broadly self-consistent state selective charge transfer cross-section database for both $n = 1$ and $n = 2$ hydrogen isotope donors for receiver charges z_r = 1-10, established for, in fact, the bare nucleus receivers H^{+1} through to Ne^{+10}. These data are most strongly influenced by close-coupled atomic orbital (CCAO) calculations in the energy regime $E_{cm} \lesssim 50$ kev/amu and by classical trajectory Monte Carlo (CTMC) calculations for $E_{cm} \gtrsim 50$ kev/amu. Recent

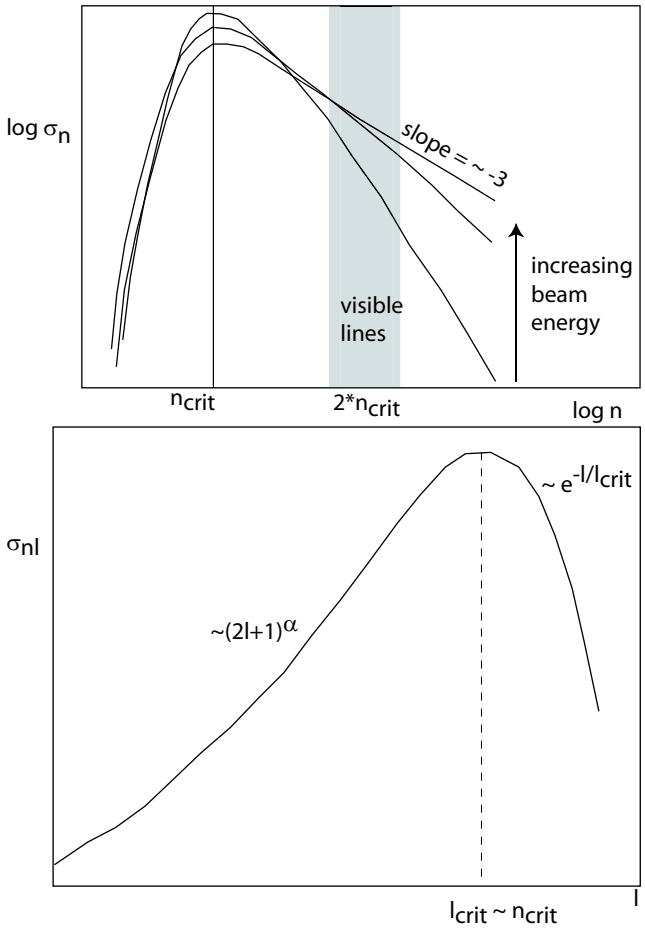

Figure 4.1: Schematic behaviour of partial charge exchange cross-sections. (a) σ_n Vs n: Note that σ_n maximises at an n_{crit} which is $\sim z_r^{3/4}$ (b) σ_{nl} Vs l: Note that σ_{nl} maximises at an l_{crit} which is $\sim n_{crit}$

.

studies on CTMC suggest that an improvement of the handling of the classical representation of the donor state in real space is necessary for $z_r \gtrsim 10$. Also, it is suggested that the improved CTMC results are valid for sub-dominant levels to lower energy, $E_{cm} \sim 10$ kev/amu, for $n = 1$ hydrogen donor than heretofore. New data has been assembled in this approximation for Ne^{+10}, Ar^{+16} and Ar^{+18}. We have used the older ADAS data up to neon and these newer additions to assess the feasibility of determining a universal z-scaled state total and state selective charge exchange cross-sections applicable to all heavy element ion receivers. ADAS archives state selective charge exchange data in the ADAS data format *adf01* . The goal of this chapter to produce datasets for any arbitrary ion in this format. This will allow progress on heavy ions for which at this stage direct computation of sophisticated charge exchange cross sections is not feasible.

4.1 The scaled total cross-section, $\bar{\sigma}_{tot}(\epsilon)$

The CX cross section data sets listed above have been used to obtain a range of CX cross section information for different z. [FIXME:comment on datasets]. The total cross section, σ_{tot}, as a function of energy is shown in figure **??**. Scaling of both σ_{tot} and E, of the form $\sigma^*_{tot} = \sigma_{tot} i z_r^{-\alpha}$, and $E^* = E \times i z_r^{-\beta}$, where α, β are constants, are found to bring the total cross sections onto a similar curve. Interpolation of these values onto a new grid of E^*, identical for each element, and selection of an appropriate α, β pair produces a universal scaled total cross section, $\sigma^u_{tot}(E^*)$. The best values of α and β can be obtained by placing a best fit curve through the scaled data, in this work this is done by eye. These results are shown in figure **??**. From these values, it is then possible to unfold to obtain $\sigma_{tot}(E)$ for any

arbitrary ion (see section **??** below).

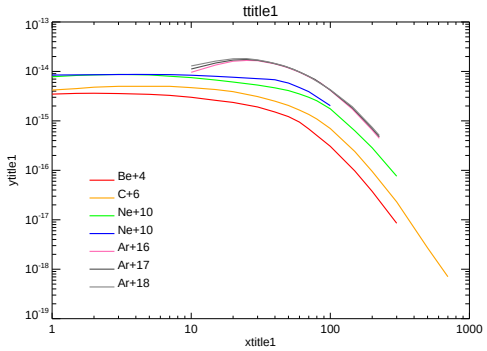
ttitle1
ytitle1
xtitle1
Be+4
C+6
Ne+10
Ne+10
Ar+16
Ar+17
Ar+18

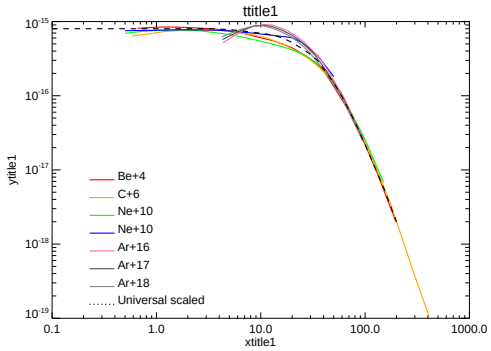
ttitle1
ytitle1
xtitle1
Be+4
C+6
Ne+10
Ne+10
Ar+16
Ar+17
Ar+18
Universal scaled

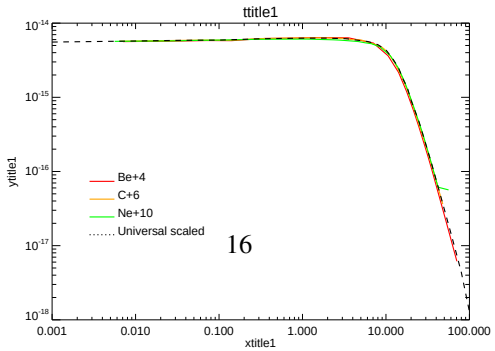
ttitle1
ytitle1
xtitle1
Be+4
C+6
Ne+10
Universal scaled

4.2 The scaled n-shell resolved cross-section, $\bar{\sigma}_\nu(\epsilon)$

Calculation of the probability of capture into each n shell of the recombining ion is required to accurately recreate the cascade which gives rise to diagnostically useful CX spectra. The n shell with the largest cross section increases with increasing recombining ion charge, iz^r. A scaling of the form $n^* = niz_r^{1\gamma(E^*)}$ is found to be suitable. Again, a similar scaling can be applied to the cross sections, $\sigma_n^* = \sigma_n iz_r^{-\kappa(E^*)}$. Both γ and κ are independent of iz^r. A typical plot of these quantites is shown in figure **??**.

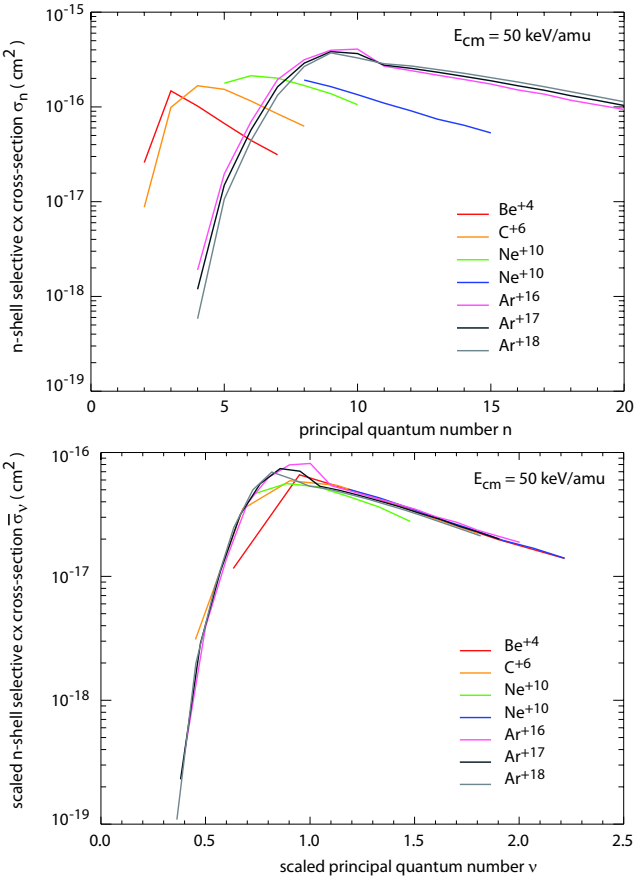

Figure 4.3: Behaviour of the n-shell selective charge exchange cross-section (a) σ_n Vs principal quantum number n for H($n = 1$) donor with various recombining ions at centre of mass collision energy E_{cm} =50keV/amu. (b) Scaled n-shell selective charge exchange cross-section $\bar{\sigma}_\nu = \sigma_n / z_r^\alpha$ Vs scaled principal quantum number $\nu = n/n_{crit}$ for hydrogen $n = 1$ donor with various recombining ions for optimised parameters α and β.

A minimisation of χ^2 method has been used to obtain the values of δ and κ which provide the best fit to the available data for each E^*. A weighted average of $\sigma_n^*(E^*, n^*)$ has been taken, then renormalised to σ_{tot}^u to provide the universal scaled n-shell resolved cross section, σ_n^u.

The weighting of the different datasets is trivial at high energy, when the scaled data show good agreement with each other, however at lower energy ($E^* < 5$kev/amu) the weightings given to each dataset require some judgement by the operator as differences between the sets rise. From this work, the constant $\beta = 0.3$; this means that $E^* < 5$kev/amu corresponds to $E < 17$kev/amu for a typical W emitting ion (W+^{64}). Tokamak CXS systems rely on charge exchange from neutral deuterium beams; current systems operate above this range (typically $E > 20$keV/amu): in ITER the diagnostic beam will operate in the $E \approx 60$keV/amu range, so the scalings presented here are acceptable for this application.

4.3 The scaled nl-shell resolved cross-section, $\bar{\sigma}_{\nu\lambda}(\epsilon)$

Extension of this work into *l* shell resolved cross sections would, in theory, be possible, however the data files generated would be prohibitively large and the improvement it would provide to the model would not neccessarily be worthwhile. For this reason, *l* shell information has not been included in the universal scalings. It is possible, however, to use existing *l* shell population codes with the *n* shell resolved data to recreate *l* shell data.[FIXME: EXAMPLE,CODE NUMBER etc?]

4.4 The code adas315 and formats adf49, adf01

The universal z-scaled charge exchange cross-section data is conveniently archived to a variant of the ADAS data format *adf01* used for light element state selective charge transfer cross-sections. This new format is given the number *adf49*. At present there are *adf49* data sets for H($n = 1$) and H($n = 2$) donors, namely:

/home/adas/adas/adf49/h0_en1_arf07.dat
/home/adas/adas/adf49/h0_en2_arf07.dat.

These data sets are created by a parametric optimised fitting code drawing on the set of *adf01* data for the specific receiver ions identified earlier in this chapter. It is anticipated that as refined calculations for other heavier ions are procured, their *adf01* files will be incorporated in revised/improved fittings and the *adf49* production repeated. The *arf07* part of the dataeset name recognises the current 2007 production by Adam Foster. An extract of the dataset for H($n = 1$) donor is shown in figure 4.5. Note the replacement of the usual integer *n* list of receiver principal qunatum shells by the non-integral scaled parameter ν. ν does not correspond to the effective principal quantum number used in atomic physics but is defined as $\nu = n/n_{crit}$.

The preparation of a *adf01* file for a specific ion from a universal *adf49* source is straightforward and available under IDL at the command line. For creation of the *adf01* file for a single ion, the procedure is

/home/adas/idl/adas3xx/adas315/adas315_make_adf01.pro

The set of IDL commands for adf01 production with Sn^{+20} as the receiver for capture from H($n = 2$) is

```
IDL>   zr0 = 50
IDL>   zr1 = 20
IDL>   adf49_file = '/home/adas/adas/adf49/h0_en2_arf07.dat'
IDL>   adf01_file = 'bn#50_en2_sn20.dat'

IDL>   adas315_make_adf01,   zr0=zr0, zr1=zr1, $
                             adf49_file=adf49_file, $
                             adf01_file=adf01_file
or

IDL>   adas315_make_adf01,   zr0=zr0, zr1=zr1, /lvalues,$
                             adf49_file=adf49_file, $
                             adf 01_file=adf01_file
```

where the first form produces only whole n-shell selective charge exchange cross-section data and the second form produces the nl-shell selective data.The resulting *adf01* file in the first case is shown in figure 4.6. The complete set of keyword parameters is given in the appendix to this report. An extended range of keyword parameters allows alteration of the default beam energy ranges and the span of n-shells. Details are in the appendix to this report. The *adf01* file is fully formed ready for subsequent use in ADAS. Archiving of the extensive data for heavy elements in central adas is in sub-directories of *adf01* as

/···/adf01/qcx#h0/bn#<zr0>/bn#<zr0>_en<nd>_<elsymb><zr1>.dat

where < *zr*0 > denotes the receiver nuclear charge, < *nd* > denotes the neutral hydrogen donor n-shell, < *elsymb* > dnotes the receiver element chemical symbol and < *zr*1 > denotes the capturing receiver ionisation stage number. It is convenient to allow mass production of all the ionisation stages of an element at once. The IDL procedure

/home/adas/idl/adas3xx/adas315/adas315.pro

allows this. The set of IDL commands for complete element *adf01* sub-library production with Sn as the receiver element for capture from H($n = 1$) in the *bn* form is

```
IDL>   zr0 = 50
IDL>   adf49_file =   '/home/adas/adas/adf49/h0_en1_arf07.dat'
IDL>   adf01_lib =    '/home/¡userid¿/adas/adf01/qcx#h0/bn#50'
IDL>   adas315,       zr0=zr0, adf49_file=adf49_file, $
                      adf01_lib=adf01_lib
```

The complete set of keyword parameters for the procedure is detailed in the appendix to this report.

4.5 The code adas316 and formats adf12, adf25 and adf26

ADAS316 performs the bundle-n populations calculations. The primary code and its subroutines are in the FORTRAN language. The organisation is shown in the schematic of figure 4.7. The code operates as a series of cycles through vectors of key plasma parameters. These are beam energy, plasma ion temperature, mean plasma ion density and z effective and the scans in these parameters are 1-dimensional scans about a reference set of conditions. The various subroutines are self-contained (see however **cgbntb.for**) and may form the components of personal codes.

The code and sub-routines reside in

/home/adas/fortran/adas3xx/adas316

The core subroutine which executes a bundle-n population calculation is **cgbnhs.for**. It is based on a representative n-shell approach which allows inclusion of very many n-shells. Originally designed for dielectronic recombination, this capability is well suited to heavy ion charge exchange where n-shell selective charge exchange cross-sections can peak at very high n. It is to be noted that the product of the bundle-n calculation is substantially more than just that required for the charge exchange effective emission coefficients. It is helpfully executed within an outer subroutine **cgbntb.for** which sorts out all useful derived quantities including the collisional-radiative recombination, ionisation and radiated power coefficients with beams switched on and off and the formal separation of the b_n factors into their $f_n^{(1)}$, $f_n^{(2)}$ and $f_n^{(3)}$ parts following equation **??**.

ADAS data format *adf25* is used for drivers of variants of bundle-n population models. A revised, more self-explanatory organisation, which will form the template for all future bundle-n developments has been used for the present work, archived as

/···/adf25/a25_p316/bn#<zr0>/bn#<zr0>_<elsymb><zr>.dat

where < *zr*0 > denotes the receiver nuclear charge, < *elsymb* > denotes the receiver element chemical symbol and < *zr* > denotes the receiver ionisation stage number after electron capture. The organisation and parameters of and *adf25/a25_p316/* driver is shown in figures 4.8, 4.9 4.10 4.11 along with descriptions of the meaning of the various plasma and control parameters.

ADAS data format *adf26* is used for archiving the complete set of derived data from **cgbntb.for**. With multiple scans implemented in **adas316.for**, these data can be very extensive and so they are restricted to just the reference plasma parameter case and are archived as

/···/adf26/a25_p316/bn#<zr0>/bn#<zr0>_<elsymb><zr>.dat

with the naming conventions as for *adf25* above. An illustration is given in figure 4.12.

The output of charge exchange effective emission coefficients of principal concern here are archived in ADAS data format *adf12*. These data are written by the subroutine **cgwr12.for** and the output datset structure is fully formed for subsequent use in ADAS. The standard archiving is as

/···/adf12/qef07#h0/bn#<zr0>/bn#<zr0>_<elsymb><zr>.dat

with the naming conventions as for *adf25* above. An illustration is given in figure 4.13. To make use of *adf12* data in user FORTRAN and IDL codes, there are standard access routines and procedures **xxdata_12.for** and **xxdata_12.pro**. Also the procedure **read_adf12.pro** allows interpolation. These access routines and procedures are considerably more complete that those previously available in ADAS. In particular, precise air wavelength is returned and the information available from the header lines as character strings are more useful. The new procedures and routines have modified call parameters, but read transparently all older forms of *adf12* datasets.

Following normal ADAS practice, an interactive code ADAS316 is provided which is activated from the ADAS series 3 menu in an interactive session.

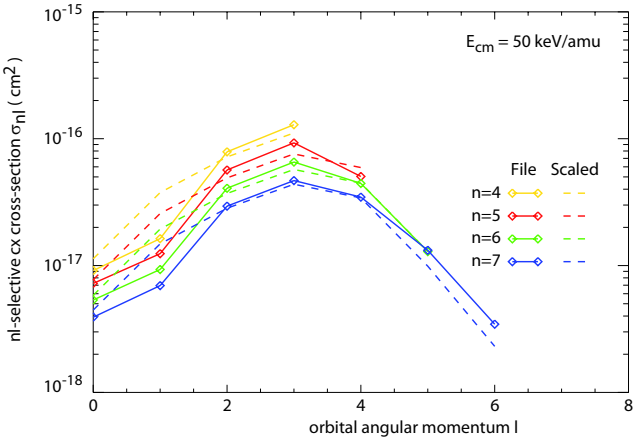

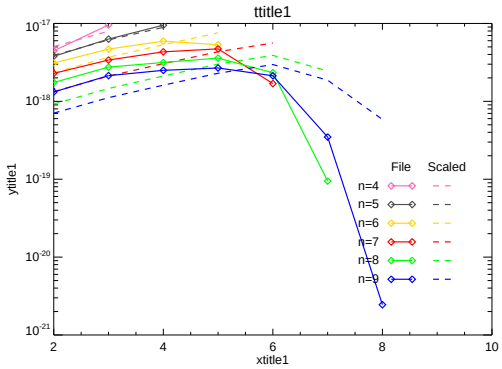

Figure 4.4: Behaviour of the nl-shell selective charge exchange cross-section (a) σ_{tot} for H($n = 1$) donor with various recombining ions. (b) Scaled total cross-section $\sigma_{tot}/z_r^{\alpha}$ Vs scaled energy E_{cm}/z_r^{β} for hydrogen $n = 1$ donor with various recombining ions for optimised parameters α and β. The final z-scaled total cross-section $\bar{\sigma}_{tot}(\epsilon)$ Vs ϵ ($= E_{cm}/z_r^{\beta}$) is the solid black line.

```
Universal H + 0 (1)  / Universal Scaled Cross Section Data    / LPARMS /
   34                / total number of scaled energies
   26                / number of scaled n shells
    1.050                / alpha
   0.3000                / beta
    7                / number of scaled energies
                     0.001000   0.01000   0.03000   0.05000    0.1000    0.3000    0.5000 / scaled energies (keV/amu)
                       0.7500    0.7500    0.7500    0.7500    0.7500    0.7400    0.7400 / gamma
                      -0.9000   -0.9000   -0.9700   -0.9000   -0.9000   -0.9000   -0.9000 / delta
                        1.000     1.000     1.000     1.000     1.000     1.000     1.000 / xlcuta_power
                       0.5000    0.5000    0.5000    0.5000    0.5000    0.5000    0.5000 / xlcuta_coeff
                        1.000     1.000     1.000     1.000     1.000     1.000     1.000 / pl2a_power
                       0.7500    0.7500    0.7500    0.7500    0.7500    0.7500    0.7500 / pl2a_coeff
                       0.5000    0.5000    0.5000    0.5000    0.5000    0.5000    0.5000 / pl3a_power
                        1.000     1.000     1.000     1.000     1.000     1.000     1.000 / pl3a_coeff
                    8.000E-16 8.000E-16 8.000E-16 8.000E-16 8.000E-16 8.000E-16 8.000E-16 / scaled total x sect (cm2)
    n*        l*                                                                          / partial x sect (cm2)
   0.2000           1.000E-40 1.000E-40 1.000E-40 1.000E-40 1.000E-40 1.000E-40 1.000E-40
   0.3000           1.000E-40 1.000E-40 1.000E-40 1.000E-40 1.000E-40 1.000E-40 1.000E-40
   0.4000           1.000E-40 1.000E-40 1.000E-40 1.000E-40 1.000E-40 1.000E-40 1.000E-40
   0.5000           1.000E-40 2.450E-31 1.790E-29 1.310E-28 1.970E-27 5.760E-25 3.180E-24
   0.6000           1.000E-40 3.430E-27 1.160E-25 5.930E-25 5.460E-24 9.190E-24 6.350E-23
   0.7000           1.000E-40 8.740E-24 1.230E-22 4.220E-22 2.240E-21 2.070E-21 9.630E-21
   0.8000           3.450E-19 5.810E-20 2.500E-19 4.920E-19 1.240E-18 7.920E-19 1.980E-18
   0.9000           2.220E-17 2.940E-17 5.690E-17 7.730E-17 1.170E-16 5.370E-17 8.830E-17
    1.000           2.170E-16 4.750E-16 6.500E-16 7.520E-16 9.170E-16 6.000E-16 7.560E-16
    1.100           3.120E-16 7.520E-16 9.480E-16 1.060E-15 1.220E-15 1.090E-15 1.270E-15
    1.200           6.940E-17 2.580E-16 3.600E-16 4.200E-16 5.180E-16 7.820E-16 9.200E-16
    1.300           1.400E-18 9.340E-18 2.130E-17 3.130E-17 5.270E-17 2.200E-16 2.980E-16
    1.400           1.820E-21 5.780E-20 2.960E-19 6.330E-19 1.780E-18 1.560E-17 3.060E-17
    1.500           1.670E-25 1.800E-21 1.490E-20 4.000E-20 1.520E-19 6.300E-19 1.980E-18
    1.600           1.000E-40 1.000E-40 1.860E-21 5.750E-21 2.660E-20 6.000E-20 2.610E-19
    1.700           1.000E-40 1.000E-40 1.000E-40 2.960E-21 1.390E-20 2.690E-20 1.220E-19
    1.800           1.000E-40 1.000E-40 1.000E-40 1.270E-21 6.420E-21 2.190E-20 9.200E-20
    1.900           1.000E-40 1.000E-40 1.000E-40 1.000E-40 3.530E-21 1.210E-20 5.090E-20
    2.000           1.000E-40 1.000E-40 1.000E-40 1.000E-40 2.040E-21 6.610E-21 2.810E-20
    2.100           1.000E-40 1.000E-40 1.000E-40 1.000E-40 1.000E-40 3.900E-21 1.660E-20
    2.200           1.000E-40 1.000E-40 1.000E-40 1.000E-40 1.000E-40 1.620E-21 7.540E-21
    2.300           1.000E-40 1.000E-40 1.000E-40 1.000E-40 1.000E-40 1.080E-21 4.980E-21
    2.400           1.000E-40 1.000E-40 1.000E-40 1.000E-40 1.000E-40 1.000E-40 2.730E-21
    2.500           1.000E-40 1.000E-40 1.000E-40 1.000E-40 1.000E-40 1.000E-40 1.490E-21
    2.600           1.000E-40 1.000E-40 1.000E-40 1.000E-40 1.000E-40 1.000E-40 1.000E-40
    2.700           1.000E-40 1.000E-40 1.000E-40 1.000E-40 1.000E-40 1.000E-40 1.000E-40

                         . . .

   -1   -1
C-----------------------------------------------------------------------------------------
C Universal scaling laws for Charge Exchange data
C Wed May 23 09:58:59 2007
C Code: write_universal_xsect.pro   Version:      1.00000
```

Figure 4.5: *adf49* table for H(n = 1) donor. The principal correspondences with the notations of the previous sections are : *scaled energy* $\equiv \epsilon$, n* $\equiv \nu$, *scaled total cross-section* $\equiv \bar{\sigma}_{tot}(\epsilon)$, *partial cross-section* $\equiv \bar{\sigma}_{\nu}(\epsilon)$. The complete specification of the format is in the appendix to this report.

```
Sn+20     H + 0 (2)  / receiver, donor (donor state index)    /        /
    9                / number of energies
    9                / nmin
   27                / nmax
            0.01     0.02     0.05     0.10     0.20     0.50     1.00     2.00     5.00 /energies
(keV/amu)
            6.88     5.39    15.30    15.27    15.34    11.35     4.23     7.59     7.58 /alpha
          1.68E-13 1.69E-13 1.72E-13 1.74E-13 1.74E-13 1.80E-13 1.83E-13 1.85E-13 1.84E-13 /total xsects.    (cm2)
  n  l  m                                                                                 /partial xsects.  (cm2)
   9        0.00E+00 0.00E+00 0.00E+00 0.00E+00 0.00E+00 0.00E+00 0.00E+00 0.00E+00 0.00E+00
  10        0.00E+00 0.00E+00 0.00E+00 0.00E+00 0.00E+00 0.00E+00 0.00E+00 0.00E+00 0.00E+00
  11        0.00E+00 0.00E+00 0.00E+00 0.00E+00 0.00E+00 0.00E+00 0.00E+00 0.00E+00 7.83E-18
  12        0.00E+00 0.00E+00 1.41E-18 1.84E-18 3.55E-18 3.08E-17 1.21E-16 1.02E-16 1.00E-16
  13        0.00E+00 0.00E+00 6.63E-18 8.23E-18 1.61E-17 1.16E-16 3.67E-16 3.04E-16 2.97E-16
  14        3.74E-17 7.16E-17 1.03E-16 1.31E-16 1.49E-16 6.00E-16 1.34E-15 1.09E-15 1.06E-15
  15        1.02E-15 1.18E-15 8.94E-16 1.04E-15 1.22E-15 2.46E-15 3.84E-15 3.09E-15 2.81E-15
  16        8.04E-15 6.36E-15 3.01E-15 3.30E-15 3.87E-15 7.03E-15 7.79E-15 6.19E-15 4.47E-15
  17        1.57E-14 1.27E-14 8.46E-15 1.01E-14 8.68E-15 1.27E-14 1.52E-14 1.03E-14 6.32E-15
  18        2.57E-14 2.17E-14 1.80E-14 2.05E-14 1.54E-14 1.90E-14 2.27E-14 1.45E-14 9.05E-15
  19        3.89E-14 3.39E-14 2.79E-14 2.57E-14 2.12E-14 2.38E-14 2.46E-14 1.72E-14 1.33E-14
  20        4.41E-14 4.25E-14 3.46E-14 3.02E-14 2.53E-14 2.50E-14 2.46E-14 1.96E-14 1.64E-14
  21        2.49E-14 3.05E-14 3.26E-14 2.89E-14 2.79E-14 2.33E-14 2.17E-14 2.06E-14 1.89E-14
  22        4.48E-15 8.53E-15 1.78E-14 1.81E-14 2.35E-14 1.74E-14 1.49E-14 1.83E-14 1.85E-14
  23        2.25E-15 4.94E-15 1.04E-14 1.19E-14 1.47E-14 1.27E-14 1.12E-14 1.63E-14 1.71E-14
  24        1.13E-15 2.86E-15 6.05E-15 7.80E-15 9.26E-15 9.30E-15 8.36E-15 1.45E-14 1.58E-14
  25        5.84E-16 1.68E-15 4.09E-15 5.44E-15 6.86E-15 7.14E-15 6.41E-15 1.15E-14 1.33E-14
  26        3.02E-16 9.84E-16 2.85E-15 3.85E-15 5.25E-15 5.53E-15 4.94E-15 8.81E-15 1.10E-14
  27        1.65E-16 6.04E-16 1.99E-15 2.73E-15 3.98E-15 4.33E-15 3.87E-15 6.81E-15 9.19E-15

                  . . .

   -1   -1
C-----------------------------------------------------------------------------------------
C Data Generated by universal scaling laws for Charge Exchange
C Date    : Fri Jun  1 16:48:12 2007
C Suthor  : afoster
C Code    : adas315.pro
C Version :      1.20000
C-----------------------------------------------------------------------------------------
```

Figure 4.6: *adf01* table for Sn^{+20} receiver ion and H(n = 2) donor. Note that only n-shell data is given in this case as keyword *lvalues* was not used in its generation. The complete specification of the format is in the appendix to this report.

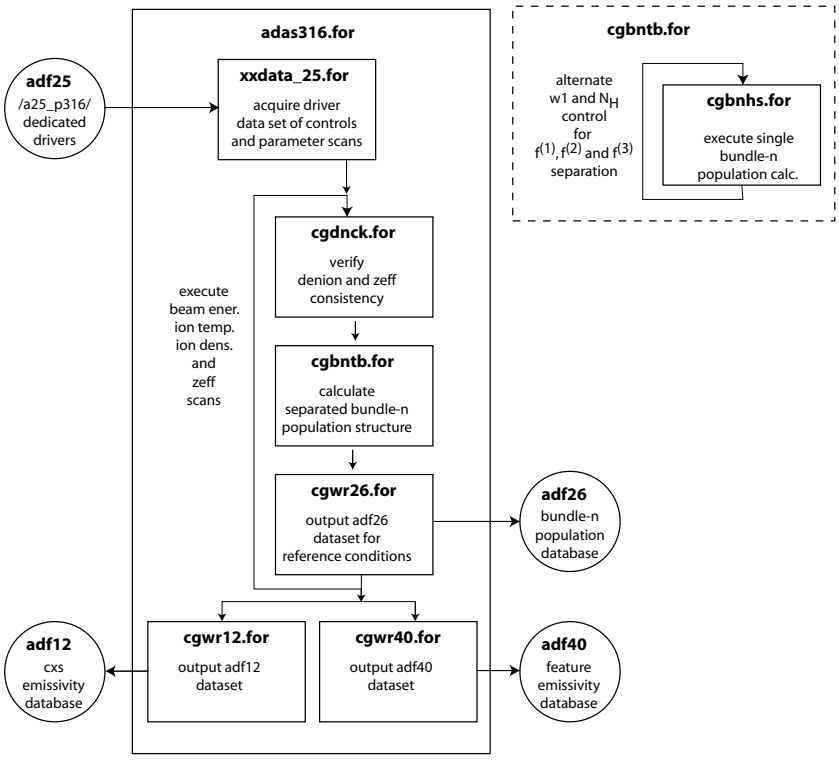

Figure 4.7: Schematic of adas316 fortran processing and subroutines.

```
receiver ion parameters
-----------------------
z0       :    6
z1       :    6
outfmt   : adf12
exfile   : /home/adas/adas/adf18/p310_a17/bndlen_exp#h0.dat
cxfile   : /home/adas/adas/adf01/qcx#h0/qcx#h0_old#c6.dat

plasma density parameters
-------------------------
ndens    :    4
id_ref   :    2
densa    :  1.00E 09  0.00E 00  0.00E 00  0.00E 00  0.00E 00  0.00E 00  0.00E 00
denpa    :  0.00E 00  0.00E 00  0.00E 00  0.00E 00  0.00E 00  0.00E 00  0.00E 00
denimpa  :  0.00E 00  0.00E 00  0.00E 00  0.00E 00  0.00E 00  0.00E 00  0.00E 00
deniona  :  1.00E 12  3.00E 12  1.00E 13  3.00E 13  0.00E 00  0.00E 00  0.00E 00

plasma temperature parameters
-----------------------------
ntemp    :    1
it_ref   :    1
tea      :  1.16E 05  0.00E 00  0.00E 00  0.00E 00
tpa      :  1.16E 05  0.00E 00  0.00E 00  0.00E 00
timpa    :  1.16E 05  0.00E 00  0.00E 00  0.00E 00
tiona    :  1.16E 05  0.00E 00  0.00E 00  0.00E 00

plasma zeff parameters
----------------------
nzef     :    4
iz_ref   :    2
zefa     :   1.00000   2.00000   3.00000   6.00000


neutral beam donor parameters
-----------------------------
nbeam    :   13                    ;
ib_ref   :    7
bmena    :  1.00E 04  1.50E 04  2.00E 04  2.50E 04  3.00E 04  3.50E 04  4.00E 04
         :  4.50E 04  5.00E 04  5.50E 04  6.00E 04  6.50E 04  7.00E 04
denha    :  1.00E 08  1.00E 08  1.00E 08  1.00E 08  1.00E 08  1.00E 08  1.00E 08
         :  1.00E 08  1.00E 08  1.00E 08  1.00E 08  1.00E 08  1.00E 08
bmfra    :  1.00E 00  1.00E 00  1.00E 00  1.00E 00  1.00E 00  1.00E 00  1.00E 00
         :  1.00E 00  1.00E 00  1.00E 00  1.00E 00  1.00E 00  1.00E 00

plasma impurity parameters
--------------------------
nimp     :    2
im_ref   :    1
zimpa    :  4.00E 00  6.00E 00
amimpa   :  8.00E 00  1.20E+01
frimpa   :  0.50E 00  0.50E 00
```

Figure 4.8: *adf25-part1*: The *outfmt* controls the use of plasma parameters.For *adf12* production, the scans use *denion* and *zef*. The plasma hydrogen isotope density (called protons) is distinguished from the other plasma impurity species. With the fractional mix of other impurities specified, the proton density *denp* and the electron density *dens* are determined from *denion* and *zef*. Values of *denp*, *dens* and *denimp* given in the driver may therefore be overwritten in this case and not all values of *zef* may be possible. Subroutine **cgdnck.for** scrutinises and truncates as required. *xxdata_25.for* provides appropriate warnings.

```
control parameters - radiation
------------------------------
ts       :  1.00E 06
w        :  0.00E 00
wl       :  1.00E 08

control parameters - collisions
-------------------------------
cion     :  1.00E 00
cpy      :  1.00E 00
nip      :    0
intd     :    3
iprs     :    1
ilow     :    1
ionip    :    0
nionip   :    2
ilprs    :    1
ivdisp   :    0

representative level parameters
-------------------------------
nmin     :    1
nmax     :  110
imax     :   22
nrep     :    1    2    3    4    5    6    7    8    9   10   11   12   15   20
         :   25   30   40   50   60   70   80   90
wbrep    :  0.00E 00  0.00E 00  0.00E 00  0.00E 00  0.00E 00  0.00E 00  0.00E 00  0.00E 00
         :  0.00E 00  0.00E 00  0.00E 00  0.00E 00  0.00E 00  0.00E 00  0.00E 00  0.00E 00
         :  0.00E 00  0.00E 00  0.00E 00  0.00E 00  0.00E 00  0.00E 00  0.00E 00  0.00E 00
         :  0.00E 00
jdef     :    1
def      :   0.00000

dielectronic recombination parameters
-------------------------------------
jcor     :    4
cor      :   0.05000   0.30000   0.70000   0.90000
jmax     :    1
epsil    :   0.75000
fij      :   0.00000
wij      :  0.00E 00

c-------------------------------------------------------------------------------
c  sample adas316 driver file of format /.../adas/adf25/p316/
c
c Notes:
c
c   input : (i*4)  iunit    = unit number for input adf01 file.
c   input : (c*8)  a25fmt   = subdirectory type of adf25 to be read.
c   input : (c*80) dsname   = file name of adf25 format to be read.
c
c   input : (i*4)  ndtem    = maximum number of electron temperatures
c   input : (i*4)  ndden    = maximum number of electron densities
c   input : (i*4)  ndrep    = maximum number of representative n-shells
c   input : (i*4)  ndcor    = maximum number of DR bethe corrections
c   input : (i*4)  nddiel   = maximum number of DR core transitions
c   input : (i*4)  nddef    = maximum number of quantum defects
c   input : (i*4)  ndimp    = maximum number of plasma impurities
c   input : (i*4)  ndlev    = maximum number of n-shells
c   input : (i*4)  ndein    = maximum number of beam energies
c   input : (i*4)  ndzef    = maximum number of z effectives
```

Figure 4.9: *adf25-part2*: The parameters *denh* and $w1$ are used to enable the separation of b_n into its $f_n^{(1)}$, $f_n^{(1)}$ and $f_n^{(3)}$ components. $w1$ is a dilution factor on a Planck radiation field of radiation temperature T_s (K) for photo-ionisation from the lowest n-shell. Such a radiation field has no relenace in the fusion case and the general dilution factor w is set to zero, but $w1$ may be used as a switch to eliminate the $f_n^{(1)}$ part. The subroutine **cgbntb.for** alternatively switches on *denh*, the neutral hydrogen beam density, and $w1$ in a set of four runs to achieve the complete separation.

```
c   input : (i*4)  iz0      - nuclear charge of bundle-n ion
c   input : (i*4)  iz1      - recombining ion charge of bundle-n ion
c   input : (c*5)  outfmt   - format of output ADAS data format for final
c                            results
c   input : (c*80) cxfile   - file name for charge exchange data input
c   input : (c*80) exfile   - file name for map of proj. matrix output
c
c   input : (i*4)  ndens    - number of electron densities
c   input : (i*4)  id_ref   - reference electron density pointer in vectors
c   input : (i*4)  densa()  - plasma electron density vector (cm-3)
c                            1st dim: index of electron density
c   input : (i*4)  denpa()  - plasma H+ density vector (cm-3)
c                            1st dim: index of electron density
c   input : (i*4)  denimpa()- plasma mean impurity ion density (cm-3)
c                            1st dim: index of electron density
c
c   input : (i*4)  ntemp    - number of electron temperatures
c   input : (i*4)  id_ref   - reference electron temp. pointer in vectors
c   input : (i*4)  tea()    - plasma electron temp. vector (K)
c                            1st dim: index of electron temperature
c   input : (i*4)  denpa()  - plasma H+ temp. vector (K)
c                            1st dim: index of electron temperature
c   input : (i*4)  denimpa()- plasma mean impurity ion temp (K)
c                            1st dim: index of electron temperature
c
c   input : (i*4)  nzef     - number of plasma zeff
c   input : (i*4)  iz_ref   - reference zeff pointer in vector
c   input : (i*4)  zefa()   - plasma zeff vector
c                            1st dim: index of zeff
c
c   input : (i*4)  nbeam    - number of beam energies
c   input : (i*4)  ib_ref   - reference beam energy pointer in vectors
c   input : (i*4)  bmena()  - beam energy vector (ev/amu)
c                            1st dim: index of beam energies
c   input : (i*4)  denha()  - beam H+ density vector (cm-3)
c                            1st dim: index of beam energies
c   input : (i*4)  bmfra()  - fractions of beam at each energy
c                            1st dim: index of beam energies
c
c   input : (i*4)  nimp     - number of plasma impurities (excl.h+)
c   input : (i*4)  im_ref   - reference impurity pointer in vectors
c   input : (r*8)  zimpa()  - impurity species charge
c                            1st dim: index of impurity
c   input : (r*8)  amimpa() - atomic mass number of impurity species
c                            1st dim: index of impurity
c   input : (r*8)  frimpa() - fraction of impurity (normalised to 1)
c                            1st dim: index of impurity
```

Figure 4.10: *adf25-part3*

```
c   input : (r*8)  ts       = external radiation field temperature (K)
c   input : (r*8)  w        = general radiation dilution factor
c   input : (i*4)  wl       = external radiation field dilution factor
c                             for photo-ionisation form the ground level.
c
c   input : (r*8)  cion     = adjustment multiplier for ground ionis.
c   input : (r*8)  cpy      = adjustment multiplier for VR xsects.
c   input : (i*4)  nip      = range of delta n for IP xsects. (le.4)
c   input : (i*4)  intd     = order of Maxw. quad. for IP xsects.(le.3)
c   input : (i*4)  iprs     = 0  => default to VR xsects. beyond nip range
c                             1  => use PR xsects. beyond nip range
c   input : (i*4)  ilow     = 0  => no special low level data accessed
c                             1  => special low level data accessed
c   input : (i*4)  ionip    = 0 =>   no ion impact collisions included
c                             1 =>ion impact excit. and ionis. included
c   input : (i*4)  nionip   = range of delta n for ion impact
c                             excitation xsects.
c   input : (i*4)  ilprs    = 0 => default to vainshtein xsects.
c                             1 => use lodge-percival-richards xsects.
c   input : (i*4)  ivdisp   = 0 => ion impact at thermal Maxw. energies
c                             1 => ion impact at displaced thermal
c                                  energies according to the neutral
c                                  beam energy parameter
c                               * if(ivdisp=0 then special low level
c                                 data for ion impact is not substituted -
c                                 only vainshtein and lodge et al.
c                                 options are open.  Electron impact
c                                 data substitution does occur.
c   input : (i*4)  nmin     = lowest n-shell for population structure
c   input : (i*4)  nmax     = highest n-shell for population structure
c   input : (i*4)  imax     = number of representative n-shells
c   input : (i*4)  nrep()   = representative n-shells
c                             1st dim: index of representative n-shell
c   input : (r*8)  wbrep()  = dilution factors for nmin->nrep() trans.
c                             1st dim: index of representative n-shell
c   input : (i*4)  jdef     = number of n-shell quantum defects
c   input : (r*8)  def()    = quantum defects for n-shells
c                             1st dim: index of n-shell quantum defects
c                                      upwards from nmin
c   input : (i*4)  jcor     = number of DR Bethe correction factors
c   input : (r*8)  cor()    = DR Bethe correction factors
c                             1st dim: index of correction factor
c   input : (i*4)  jmax     = number of DR core transitions
c   input : (r*8)  epsil()  = reduced energy of core transition
c                             [delta Eij/I_H=(z+1)^2*epsil()]
c                             1st dim: index of DR core transition
c   input : (r*8)  fij()    = absorption oscillator strength for
c                             DR core transition
c                             1st dim: index of DR core transition
c   input : (r*8)  wij()    = dilution factor for DR core transition
c                             1st dim: index of DR core transition
```

Figure 4.11: *adf25-part4*

```
effective contribution table for ion principal quantum shell populations in thermal plasma

  CARBON                  z0 =  6                   z1 =  6

   trad = 1.00E+06 k       te = 1.16E+05 k       tp = 1.16E+05 k       timp = 1.16E+05 k       tion = 1.16E+05 k
      w = 0.00E+00         ne = 3.71E+12 cm-3     np = 2.82E+12 cm-3   denimp = 1.76E+11 cm-3   denion = 3.00E+12 cm-3

     eh = 4.00E+04 ev/amu   nh = 1.00E+08 cm-3       nh/ne = 2.70E-05   flux = 2.77E+16 cm-2 sec-1


charge exchange off : n1/n+ = 2.51820E+20  recomb coeff = 6.30196E-12 cm+3 sec-1   ioniz coeff = 2.50257E-32 cm+3 sec-1

charge exchange on  : n1/n+ = 1.00009E+21  recomb coeff = 2.50279E-11 cm+3 sec-1   ioniz coeff = 2.50257E-32 cm+3 sec-1

                      plt = 6.99678E-42 w cm+3        prb = 5.02888E-28 w cm+3         prc = 5.15696E-23 w cm+3

  i    n             f1           f2           f3          b(check)      b(actual)      nn/(bn*n+)
  1    1          1.34925E-11   0.00000E+00   0.00000E+00   1.34937E+10   1.34937E+10   7.41177E+10
  2    2          2.22612E-20   4.42426E-07   5.33388E-02   2.22632E+01   2.22632E+01   3.24749E-05
  3    3          1.33391E-20   4.67143E-04   9.00108E+01   1.33432E+01   1.33432E+01   8.09271E-08
  4    4          1.13239E-20   6.14997E-03   2.18587E+03   1.13900E+01   1.13900E+01   1.32892E-08
  5    5          1.07285E-20   2.20084E-02   6.37896E+03   1.09236E+01   1.09236E+01   6.89454E-09
  6    6          1.04913E-20   4.63917E-02   1.06833E+04   1.08270E+01   1.08270E+01   5.45472E-09
  7    7          1.03446E-20   7.55130E-02   1.22607E+04   1.07519E+01   1.07519E+01   5.17411E-09
  8    8          1.02126E-20   1.06604E-01   1.24554E+04   1.06563E+01   1.06563E+01   5.34603E-09
  9    9          1.00716E-20   1.38274E-01   1.18616E+04   1.05309E+01   1.05309E+01   5.76170E-09
 10   10          9.91031E-21   1.70677E-01   1.10243E+04   1.03794E+01   1.03794E+01   6.34086E-09
 11   11          9.71565E-21   2.03830E-01   1.00930E+04   1.01927E+01   1.01927E+01   7.04696E-09
 12   12          9.46152E-21   2.39870E-01   9.13078E+03   9.94864E+00   9.94864E+00   7.86116E-09
 13   15          7.99369E-21   3.89698E-01   6.20673E+03   8.55160E+00   8.55160E+00   1.08669E-08
 14   20          3.84186E-21   7.22249E-01   2.30468E+03   4.62665E+00   4.62665E+00   1.75632E-08
 15   25          1.54118E-21   8.91844E-01   7.99201E+02   2.45473E+00   2.45473E+00   2.62586E-08
 16   30          6.40175E-22   9.56071E-01   2.97085E+02   1.60432E+00   1.60432E+00   3.69173E-08
 17   40          1.48546E-22   9.90044E-01   6.16367E+01   1.14027E+00   1.14027E+00   6.40859E-08
 18   50          4.50423E-23   9.97023E-01   1.75693E+01   1.04254E+00   1.04254E+00   9.90363E-08
 19   60          1.61630E-23   9.98942E-01   6.06694E+00   1.01527E+00   1.01527E+00   1.41761E-07
 20   70          6.20597E-24   9.99597E-01   2.25242E+00   1.00586E+00   1.00586E+00   1.92257E-07
 21   80          2.19358E-24   9.99860E-01   7.52521E-01   1.00207E+00   1.00207E+00   2.50523E-07
 22   90          3.66715E-25   9.99979E-01   8.04187E-02   1.00035E+00   1.00035E+00   3.16559E-07


                                  bn = f1*(n1/n+) + f2 + f3*(nh/ne)
                                  n1 = population of ground state of ion
                                  n+ = population of ground state of next ionisation stage
                                  nn = population of principal quantum shell n of ion
                                  bn = saha-boltzmann factor for principal quantum shell n
                                  eh = neutral hydrogen beam energy
                                   w = radiation dilution factor
                                  z0 = nuclear charge
                                  z1 = ion charge+1

nip   = 0    intd  =  3    iprs  =  1    ilow  =  1    ionip =  0    nionip=  2    ilprs =  1    ivdisp=  0
zeff  = 2.0    ts  =  1.00E+06     w   =  0.00E+00     cion  =1.0     cpy =1.0     wl  =  1.00E+08     zimp  = 4.0 (  5.00E-01)
                                                                                                      6.0 (  5.00E-01)
```

Figure 4.12: *adf26*

```
  110
E=c   W= 3433.95 D=h(ls) R=c+6   N=7-6     F=cxs_c5_tst M=cx   isel=   1
  1.21E-07                                                     qefref
  4.00E+04  1.00E+01  3.00E+12  2.00E+00  3.00E+00             parmref
       13         1         4         3         1             nparmsc
  1.00E+04  1.50E+04  2.00E+04  2.50E+04  3.00E+04  3.50E+04   ener
  4.00E+04  4.50E+04  5.00E+04  5.50E+04  6.00E+04  6.50E+04
  7.00E+04
  5.94E-09  1.18E-08  3.10E-08  5.66E-08  8.07E-08  1.03E-07   qener
  1.21E-07  1.35E-07  1.40E-07  1.38E-07  1.33E-07  1.28E-07
  1.22E-07
  1.00E+01                                                     tiev
  1.21E-07                                                     qtiev
  1.00E+12  3.00E+12  1.00E+13  3.00E+13                       densi
  1.22E-07  1.21E-07  1.21E-07  1.20E-07                       qdensi
  1.00E+00  2.00E+00  3.00E+00                                 zeff
  9.84E-08  1.21E-07  1.59E-07                                 qzeff
  3.00E+00                                                     bmag
  1.21E-07                                                     qbmag
E=c   W= 5290.87 D=h(ls) R=c+6   N=8-7     F=cxs_c5_tst M=cx   isel=   2
  8.65E-08                                                     qefref
  4.00E+04  1.00E+01  3.00E+12  2.00E+00  3.00E+00             parmref
       13         1         4         3         1             nparmsc
  1.00E+04  1.50E+04  2.00E+04  2.50E+04  3.00E+04  3.50E+04   ener
  4.00E+04  4.50E+04  5.00E+04  5.50E+04  6.00E+04  6.50E+04
  7.00E+04
  2.55E-09  5.99E-09  1.32E-08  2.47E-08  4.16E-08  6.40E-08   qener
  8.65E-08  1.02E-07  1.09E-07  1.11E-07  1.10E-07  1.08E-07
  1.05E-07
  1.00E+01                                                     tiev
  8.65E-08                                                     qtiev
  1.00E+12  3.00E+12  1.00E+13  3.00E+13                       densi
  8.68E-08  8.65E-08  8.58E-08  8.46E-08                       qdensi
  1.00E+00  2.00E+00  3.00E+00                                 zeff
  7.01E-08  8.65E-08  1.13E-07                                 qzeff
  3.00E+00                                                     bmag
  8.65E-08                                                     qbmag

                              . . .

c-------------------------------------------------------------------------------
c  Effective coefficient list:
c
c     isel    type      ion       transition   wavln.(A)   emis. rank
c     ----    ----      ---       ----------   ---------   ----------
c
c       1.   cx.emis.  c + 5      n =  7-  6    3433.95         1
c       2.   cx.emis.  c + 5      n =  8-  7    5290.87         2

                         . . .

c     109.   cx.emis.  c + 5      n = 40- 14    5652.64       109
c     110.   cx.emis.  c + 5      n = 40- 15    6625.87       107
c
c
c  Bundle-n population code parameters:
c
c    nip   =  0     intd  =  3     iprs  =  1     ilow  =  1
c    ionip =  0     nionip=  2     ilprs =  1     ivdisp=  0
c    cion  = 1.0    cpy   = 1.0
c
c    ts(K)   =  1.00E+06     w       =  0.00E+00     w1      =  1.00E+08
c
c    zimp(1) =  4.00E+00     amimp(1)=  8.00E+00     frimp(1)=  5.00E-01
c    zimp(2) =  6.00E+00     amimp(2)=  1.20E+01     frimp(2)=  5.00E-01
c
c
c  Adf25 file : /home/summers/adas_dev/adas/adf25/a25_p316/bn_cxs_c5_tst.dat
c  Code       : adas316
c  Producer   : Hugh Summers
c  Date       : 01-06-07
c
c-------------------------------------------------------------------------------
```

Figure 4.13: *adf12*

Chapter 5

ADAS codes and data formats for level 1 and level 2 modelling

Appendix A

ADAS data formats

A.1 *adf00*: configurations and ionisation potentials

The basic data sets, of stage-to-stage form provide the ground configurations and ionisation potentials of every ion of every element up to lead. There is a second category of metastable resolved LS type which include metastable configurations and excitation energies between metastables as well as ionisation energies.

Data mnemonic:
Data root: **/home/adas/adas/adf00/**
Last update: Jan 18, 2007
Utilising subroutines: **xxdata_00.for**

Formatted files to adf00 specification:

Element	Members	Datasets	Quality
<elem. symbol>	H - Pb	<elem. Symbol>.dat	medium/high
<elem. symbol>	H - Ne, Ar	<elem. Symbol>_ls.dat	high

Notes: The format leaves open the opportunity for a intermediate coupling, J-resolved metastable form as <**elem. symb**>_**ic.dat**. GCR modelling in ADAS at this time only extends to LS resolved. The presently extended format is designed to support the needs of 'superstaging'. Spread sheet analyses of the metastable definitions and energy determinations are available and may be provided on request in the **/adf00** directory.

Data lines (stage to stage form):

Data lines	Format
ELEMENT, IZ0S	1a16,1i5
for I=0,|IZ0S|-1	
if (IZ0S.lt.0) then	
IZ, EION(I+1),CFG(I+1)	i2,1f16.8,1a120
else	
IZ,CFG(I+1)	i2,1a120
endif	
endfor	

Variable identification:

Name	Meaning	Comment
ELEMENT	element name	
IZ0S	signed nuclear charge	<0 => data lines include ionisation potential >0 => data lines do not include ionisation potential)
IZ	ion charge	
EION()	ionisation potential	eV
CFG()	configuration string	note precise formatting with 5 character space allocation to each shell

Sample 1: **/home/adas/adas/adf00/ne.dat**

```
.
neon              -10
 0  2.15650000d+01  1s2  2s2  2p6
 1  4.09640000d+01  1s2  2s2  2p5
 2  6.34600000d+01  1s2  2s2  2p4
 3  9.70800000d+01  1s2  2s2  2p3
 4  1.26220000d+02  1s2  2s2  2p2
 5  1.57930000d+02  1s2  2s2  2p1
 6  2.07280000d+02  1s2  2s2
 7  2.39100000d+02  1s2  2s1
 8  1.19583000d+03  1s2
 9  1.36221000d+03  1s1

C-----------------------------------------------------------------------
C
C Ionisation potentials : R L Kelly, J. Phys. Chem. Ref. Data,
C                                    vol. 16, Suppl. 1, 1987
C
C Update : Martin O'Mullane
C Date   : 10-09-2003
C
C-----------------------------------------------------------------------
```

Data lines (metastable resolved LS form):

Data lines	Format
ELEMENT, IZ0S (ICNCTV(k),k=0,|IZOS|-1)	1a16,1i5,30i3
for I=0,|IZ0S|-1	
IZ, EION(I+1),CFG(I+1)	i2,3x,1f16.8,1a120
for IM=1,ICNCTV(IZ+1)	
IM,EXM(I+1,IM),CFGM(I+1,IM)	2x,i3,1f16.8,1a120
endfor	
endfor	

Variable identification:

Name	Meaning	Comment
ELEMENT	element name	
IZ0S	signed nuclear charge	<0 => data lines include ionisation potential >0 => data lines do not include ionisation potential)
ICNCTV()	connection vector	number of designated metastables in each ionisation stage
IZ	ion charge	
EION()	ionisation potential	eV
CFG()	configuration string	note precise formatting with 5 character space allocation to each shell
IM	metastable index	
EXM(,)	metast/excit energy	relative to lowest metastable (the ground)of the stage (eV).
CFGM(,)	configuration string	precise formatting with 5 character space allocation to each shell.

Sample 2: **/home/adas/adas/adf00/ne_ls.dat**

```
.
neon              -10  2  2  4  3  4  2  2  1  2  1
 0     2.15967924d+01  1s2  2s2  2p6
    1  0.00000000d+00  1s2  2s2  2p6
    2  1.66470225d+01  1s2  2s2  2p5  3s1
 1     4.09699588d+01  1s2  2s2  2p5
    1  0.00000000d+00  1s2  2s2  2p5
    2  2.71747667d+01  1s1  2s2  2p4  3s1
 2     6.33840596d+01  1s2  2s2  2p4
    1  0.00000000d+00  1s2  2s2  2p4
    2  3.16459061d+00  1s2  2s2  2p4
    3  6.87319961d+00  1s2  2s2  2p4
    4  3.83810996d+01  1s2  2s2  2p3  3s1
 3     9.72103044d+01  1s2  2s2  2p3
    1  0.00000000d+00  1s2  2s2  2p3
    2  5.11466800d+00  1s2  2s2  2p3
    3  7.74145333d+00  1s2  2s2  2p3
 4     1.26230662d+02  1s2  2s2  2p2
    1  0.00000000d+00  1s2  2s2  2p2
    2  3.66216556d+00  1s2  2s2  2p2
    3  7.83077556d+00  1s2  2s2  2p2
    4  1.08614956d+01  1s2  2s1  2p3
 5     1.57822833d+02  1s2  2s2  2p1
    1  0.00000000d+00  1s2  2s2  2p1
    2  1.24081333d+01  1s2  2s1  2p2
 6     2.07270600d+02  1s2  2s2
```

```
    1  0.00000000d+00  1s2  2s2
    2  1.39122533d+01  1s2  2s1 2p1
 7     2.39096900d+02  1s2  2s1
    1  0.00000000d+00  1s2  2s1
 8     1.19582200d+03  1s2
    1  0.00000000d+00  1s2
    2  79.0507720d+02  1s1  2s1
 9     1.36219860d+03  1s1
    1  0.00000000d+00  1s1

C-----------------------------------------------------------------------
C
C Ionisation potentials : NIST  http://physics.nist.gov/
C                               PhysRefData/ASD/levels_form.html
C
C Excitation energies   : NIST  http://physics.nist.gov/
C                               PhysRefData/ASD/levels_form.html
C
C Update : Hugh Summers
C Date   : 05-01-2007
C
C-----------------------------------------------------------------------
```

A.2 *adf01*: bundle-n and bundle-nl charge exchange cross-sections

The data sets provide total, nl-resolved and arbitrarily m-resolved charge exchange cross-sections up to high n-shells of an ion. Optionally parametrisations may be given for l-subshell cross-section dependence for asymptotic behaviour. Formatting conventions and variable storage are given below. Some additional data for positive ion impact excitation of a target neutral has been included in this data class. The appropriate sub-libraries are of the form /qex#. This is a temporary decision at this time. Utilising subroutine ADAS301 interrogates such data but further processing is not meaningful at this stage.

Data mnemonic: qcx
Data root: **/home/adas/adas/adf01/**
Last update: Jun 16, 2010
Utilising subroutines: **xxdata_01.for**

Formatted files to adf01 specification:

Donor	Prefix	Members	Library	Comments	Quality
h0	e2p	h1	qcx#h0	2p donor	low
h0	e2s	h1	qcx#h0	2s donor	low
	en2_kvi	he2,li3,be4,b5,c6 ne10	qcx#h0	nl, Hoekstra, Bliek, Olson, H(n=2) donor	medium
	ex2	c6	qcx#h0	n=2 donor	low
	ex3	h1,c6	qcx#h0	n=3 donor	low
	ex4	c6	qcx#h0	n=4 donor	low
	exk	be2,be4,c4,c6,he2,o6	qcx#h0	n=2 donor, various	varied
	gyt	b5,be4,c6,h1,he2,li3, n7,o8	qcx#h0	nlm, Gayet - high energy	medium
	ofr	c6,he2,o8	qcx#h0	nl, Fritsch - from l parms.	medium
	old	b5,be4,c6,h1,he2, n7,ne10,o8,si14	qcx#h0	nl, preferred - from l parms	medium/high
	omo	c6,o8	qcx#h0	nl, CCMO - from l parms.	medium
	ool	c6,o8	qcx#h0	nl, Olson - from l parms.	medium
	ory	b5,be4,c6,h1,he2, ne10,o8,si14	qcx#h0	nl, Ryufuku - from l parms.	medium
	tmp	ar18	qcx#h0	nl, Olson	low/incomplete
he0	2s-s_kvi	he2,c6	qcx#he0	nl, Hoekstra, Turkstra, Lubinski, Olson	medium
	2s-t_kvi	he2,c6	qcx#he0	nl, Hoekstra, Turkstra, Lubinski, Olson	medium
	gyt	b5,be4,c6,h1,he2,li3, n7,o8	qcx#he0	nlm, Gayet - high energy	medium
	kvi	h1,he2	qcx#he0	nl, Hoekstra - assessed	high
	ofr	be4,c6,he2,o8	qcx#he0	nl, Fritsch - h0 transfer	low
	old	b5,be4, c6, he2, n7,ne10,o8	qcx#he0	nl, preferred - h0 transfer	low/medium
	omo	c6,o8	qcx#he0	nl, CCMO - h0 transfer	low
	ool	c6,o8	qcx#he0	nl, Olson - h0 transfer	low
	ory	b5,be4,c6,he2, ne10,o8	qcx#he0	nl, Ryufuku - h0 transfer	low
he0	1s-s_kvi	h1	qex#he0	nl, Hoekstra, Turkstra, Lubinski	medium
he1	gyt	b5,be4,c6,h1,he2,li3, n7,o8	qcx#he1	nlm, Gayet - high energy	medium
li0	kvi	he2,li3,be4,b5,c6,n7, o8,ne10	qcx#li0	nl, Hoekstra,Bliek, Olson	medium
na0	kvi	he2	qcx#na0	nl, Hoekstra/Shingal	high

Notes:

1. When the first letter of the prefix is ‘o’, it indicates that the data has been converted from the orginal JET prescription for this data class to the present prescription. The original prescription stored n-shell data with a fitted formula for the l-distribution. The formula has been used to reconstitue the explicit nl-shell data for the present prescription.

2. h0 transfer indicates that there was no specific data for this donor. The data set has been created by formulaic conversion of the corresponding h0 donor data. Limited spot checks have indicated that this conversion is remarkably accurate.

3. The prefix ‘en..’ indicates charge transfer data from excited donor states.

4. The prefices ‘1s-s’, ‘2s-s’ and ‘2s-t’ indicate donation from the 1s2 ^{1}S, 1s2s 1^{1}S and 1s2s ^{3}S metastables respectively.

Data lines (stage to stage form):

Data lines	Format
RELEM, IZR, DELEM, IZD, LVLD, ... /LPARMS/	1a2,1x,1a2,5x,1a2,1x,1a2,2x,1a1
do until NENER.eq.-1	
NENER	1x,1i4
NMIN	1x,1i4
NMAX	1x,1i4
(ENER(IE), IE = 1, NENER)	10x,9f9.2
(BETA(IE), I = 1, NENER)	10x,9f9.2
if LPARMS is set	
(LTYP(IE), I = 1, NENER)	10,9i9
(XLCR(IE), I = 1, NENER)	10x,9f9.2
(PL2A(IE), I = 1, NENER)	10x,9f9.2
(PL3A(IE), I = 1, NENER)	10x,9f9.2
endif	
(OMTOT(IE), IE = 1, NENER)	10x,1p,9d9.2
for IN = NMIN to NMAX	
(OMN(IN,IE), IE = 1, NENER)	10x,1p,9d9.2
for IL = 0 to IN-1	
(OMNL(IN,IL,IE), IE=1,NENER)	10x,1p,9d9.2
repeat	
endfor	
enddo	

Variable identification:

Name	Meaning	Comment
RELEM	receiving element symbol	
IZR	receiving ion charge	
DELEM	donor element symbol	
IZD	donor atom (ion) charge	
LVLD	donor atom (ion) state index	
NENER	number of beam energies in subtable block	
NMIN	lowest n-shell for which data is included	
NMAX	largest n-shell for which data is included	
ENER()	beam energy (ev/amu)	
BETA()	power for n-shell xsect. extrapolation	
LTYP()	type of fitting for l-shell distribution	
XLCR()	critical l for the fitting (non-integral)	
PL2A()	parameter of l-shell fitting	
PL3A()	parameter of l-shell fitting	
OMTOT()	total charge transfer cross-section (cm**2)	
OMN(,)	charge transfer cross-section for n-shell	
	1st parameter - n-shell index	
	2nd parameter - energy index	
OMNL(,,)	charge transfer cross-section for nl-shell	
	1st parameter - n-shell index	
	2nd parameter - l-shell index	
	3rd parameter - energy index	
OMNLM(,,,)	charge transfer cross-section for nlm-shell	
	1st parameter - n-shell index	
	2nd parameter - l-shell index	
	3rd parameter - m-shell index	
	4th parameter - energy index	

Sample 1: **/home/adas/adas/adf00/ne.dat**

```
.
He+ 2     H + 0 (2) / receiver, donor (donor state n=2)       /        /
    9               / number of energies
    2               / nmin
    5               / nmax
              0.01     0.02     0.05     0.10     0.20     0.50     1.00     2.00     5.00 / energies
             17.00    16.20    15.00    13.86    12.68    11.00     9.65     8.30     5.85 / alpha
          1.11E-14 1.18E-14 1.18E-14 1.16E-14 1.16E-14 1.29E-14 1.30E-14 1.34E-14 1.34E-14 / total xs
  n  l  m                                                                                  / partial
  2        0.00E+00 0.00E+00 0.00E+00 0.00E+00 2.75E-18 1.01E-17 1.77E-17 4.81E-17 9.32E-17
  2  0     0.00E+00 0.00E+00 0.00E+00 0.00E+00 2.20E-18 5.07E-18 7.60E-18 1.22E-17 3.09E-17
  2  1     0.00E+00 0.00E+00 0.00E+00 0.00E+00 5.50E-19 5.07E-18 1.01E-17 3.60E-17 6.23E-17

. . .

  5        1.50E-17 2.60E-17 5.30E-17 9.00E-17 1.60E-16 3.09E-16 5.50E-16 9.00E-16 1.55E-15
  5  0     0.00E+00 0.00E+00 0.00E+00 0.00E+00 0.00E+00 0.00E+00 0.00E+00 0.00E+00 0.00E+00
  5  1     0.00E+00 0.00E+00 0.00E+00 0.00E+00 0.00E+00 0.00E+00 0.00E+00 0.00E+00 0.00E+00
  5  2     0.00E+00 0.00E+00 0.00E+00 0.00E+00 0.00E+00 0.00E+00 0.00E+00 0.00E+00 0.00E+00
  5  3     0.00E+00 0.00E+00 0.00E+00 0.00E+00 0.00E+00 0.00E+00 0.00E+00 0.00E+00 0.00E+00
  5  4     0.00E+00 0.00E+00 0.00E+00 0.00E+00 0.00E+00 0.00E+00 0.00E+00 0.00E+00 0.00E+00
    9               / number of energies
    2               / nmin
    5               / nmax
             10.00    15.00    20.00    25.00    30.00    35.00    40.00    45.00    50.00 / energies
              2.60     1.75     1.52     1.62     1.73     1.82     1.90     1.98     2.05 / alpha
          9.47E-15 4.87E-15 2.29E-15 1.14E-15 6.06E-16 3.37E-16 2.05E-16 1.28E-16 8.48E-17 / total xs
  n  l  m                                                                                  / partial
  2        1.79E-16 1.91E-16 1.31E-16 8.95E-17 6.40E-17 4.49E-17 3.15E-17 2.35E-17 1.69E-17
  2  0     6.08E-17 4.28E-17 2.56E-17 1.48E-17 9.78E-18 6.86E-18 4.61E-18 3.55E-18 2.47E-18
  2  1     1.18E-16 1.48E-16 1.05E-16 7.47E-17 5.42E-17 3.80E-17 2.69E-17 1.99E-17 1.44E-17



  5        1.58E-15 7.44E-16 3.37E-16 1.57E-16 7.75E-17 4.14E-17 2.36E-17 1.45E-17 9.05E-18
  5  0     0.00E+00 0.00E+00 0.00E+00 0.00E+00 0.00E+00 0.00E+00 0.00E+00 0.00E+00 0.00E+00
  5  1     0.00E+00 0.00E+00 0.00E+00 0.00E+00 0.00E+00 0.00E+00 0.00E+00 0.00E+00 0.00E+00
  5  2     0.00E+00 0.00E+00 0.00E+00 0.00E+00 0.00E+00 0.00E+00 0.00E+00 0.00E+00 0.00E+00
  5  3     0.00E+00 0.00E+00 0.00E+00 0.00E+00 0.00E+00 0.00E+00 0.00E+00 0.00E+00 0.00E+00
  5  4     0.00E+00 0.00E+00 0.00E+00 0.00E+00 0.00E+00 0.00E+00 0.00E+00 0.00E+00 0.00E+00
    2               / number of energies
    2               / nmin
    5               / nmax
             75.00   100.00                                                           / energies
              2.25     2.40                                                           / alpha
          1.60E-17 5.03E-18                                                           / total xs
  n  l  m                                                                             / partial
  2        4.50E-18 1.68E-18
  2  0     7.43E-19 3.36E-19
  2  1     3.76E-18 1.34E-18

. . .

  5        1.42E-18 3.69E-19
```

```
  5  0     0.00E+00 0.00E+00
  5  1     0.00E+00 0.00E+00
  5  2     0.00E+00 0.00E+00
  5  3     0.00E+00 0.00E+00
  5  4     0.00E+00 0.00E+00
C-----------------------------------------------------------------------------------------------------
C  Source:  The data consists of results of CTMC calculations made at the University of Missouri over
C              the period 1995-97.
C
C  Comments:  At this time, no direct comparison with other results is available for checking the
C             quality of the nl selective cross-sections except for Li+3 for which results are given
C             in a recent hidden curve crossing calculation by Janev et al. (1996).  Large differences
C             are observed in both the magnitude and energy dependence.  From inspection of the total
C             cross-sections, we have the strong impression that the CTMC data should be preferred.
C             In a plot of the scaled total one-electron capture cross-sections (sigma_tot(16q)^-1)
C             versus scaled energy (4Eq^-1/2), the total cross-sections should be approximately the
C             same for all systems (Janev, 1991) at least for q>3.  In these scaled units, a
C             recommendation by Janev and Smith (1995) has been presented.  The CTMC data are all clos
C             to this curve except at lower energies.  The hidden curve crossing data for Li+3 deviate
C             from this curve.  Molecular orbital calculations by Errea et al. (1996) for B+5 are in
C             good agreement with the corresponding CTMC data.  For He+2, the recommendation of Janev
C             and Smith is based on the calculations of Harel and Jouin (1990) and it is completely
C             different from the CTMC results for He+2, especially at the lower energies.  A reason
C             for this huge difference is hard to see.  It may be the extremely strong resonant
C             nature of the electron capture at low collision energies.  Resonant transfer from H(n=2)
C             in collsions with He+2 would necessarily mean that the electron ends up exactly between
C             the n=3 and n=4 levels of He+1.  Therefore electron capture may be blocked. To what exte
C             this is well described by the CTMC method is still a point of discussion.  For higher
C             charged receiver ions, levels are resonantly present.  Except for He+2 at low energies,
C             we recommend use of the present CTMC data.
C
C             The data was assembled as ADAS data files of type adf01 at JET Joint Undertaking in the
C             period 2-3 June 1997.
C
C  Authors:  F. W. Bliek*, R. Hoekstra*, R. E. Olson#
C                  * KVI, Groningen, Netherlands
C                  # University of Missouri, Rolla, USA.
C
C  Date:  9 June 1997.
C
C  Updates:
C
C-----------------------------------------------------------------------------------------------------
```

Appendix B

IDL procedures

Procedure	Current location	Local checks			Central ADAS	
		Txt	Opr	Lnk	CVS	Rel
read_adf01.pro	/home/hps/adas_dev/idl/read_adf/	y	n	n	n	n
xxdtes.pro	/home/summers/adas_dev/idl/adaslib/atomic/	y	n	n	n	n

Appendix C

FORTRAN subroutines

Subroutine	Current location	Local checks			Central ADAS	
		Txt	Opr	Lnk	CVS	Rel
xxdata_00.for	/home/hps/adas_dev/fortran/adaslib/read_adf/	y	n	n	n	n
xxdata_09.for	/home/hps/adas_dev/fortran/adaslib/read_adf/	y	n	n	n	n

Appendix D

Shell scripts

Script	Current location	Local checks			Central ADAS	
		Txt	Opr	Lnk	CVS	Rel
run_archive_808_scripts.pl	/home/hps/adas_dev/idl/adaslib/read_adf/	y	n	n	n	n
run_archive_808_paper.pl	/home/hps/adas_dev/idl/adaslib/read_adf/	y	n	n	n	n

Index